Science and Technology for Energy Transition **81**, 7 (2026)

https://doi.org/10.2516/stet/2026009

Enabling Technologies for the Integration of Electrical Systems in Sustainable Energy Conversion
Edited by Yacine Amara

Available online at:
stet-review.org

Regular Article OPEN ACCESS

Bio-inspired Novel Liver Cancer algorithm for solving large-scale combined heat and power economic dispatch problems

Swathi Polasa*, and Harish Pulluri*

Department of Electrical and Electronics Engineering, School of Engineering, Anurag University, Hyderabad 500088, Telangana, India

Received: 6 May 2024 / Accepted: 3 February 2026

Abstract. The potential of Combined Heat and Power (CHP) systems to enhance the economics and sustainability of the electricity system is garnering increasingly attention. The fact that these systems can have numerous generation units whose functions are controlled by intricate non-linear physics makes it challenging to determine how to operate them optimally. The complex interconnections within bulk power systems pose significant challenges in solving economic dispatch problems, particularly in large-scale Combined Heat and Power Economic Dispatch (CHPED) scenarios, which are difficult to address due to intricate thermal and electrical connections in cogeneration units. The current research work proposed a bio-inspired novel Liver Cancer Algorithm (LCA) to optimize a large-scale CHP economic dispatch system. The LCA algorithm employs genetic operators and a Random Opposition-Based Learning (ROBL) technique to effectively achieve a balance between local and global searches and thoroughly explore the search space. The mutation rate is adjusted based on the number of iterations, and the higher mutation rate facilitates the exploration of promising new locations and protects the algorithm from being trapped at a local minimum. Hence, a better optimum value can be achieved in less time. To investigate performance, the proposed method has been demonstrated on CHPED problems involving one medium and two different large-scale test systems, 48, 96, and 192 units, respectively, and the results were compared to other state-of-the-art powerful approaches. The experimental results indicated that the LCA algorithm surpasses other methods in solving medium and large-scale CHPED problems.

Keywords: Cogeneration, Combined heat and power (CHP), CHP economic dispatch (CHPED), Liver cancer algorithm (LCA), Levy's flight function, Random opposition-based learning (ROBL), Genetic operators.

Nomenclature

CHP	Combined Heat and Power
CHPED	Combined Heat and Power Economic Dispatch
TVAC-PSO	Particle Swarm Optimization with Time-Varying Acceleration Coefficients
OTLBO	Oppositional Teaching Learning-Based Optimization Algorithm
DRL-CSO	Deep Reinforcement Learning Based Crisscross Optimization Algorithm
NDIDE	Neighborhood-Based Differential Evolution Algorithm With A Direction-Induced Strategy
TVAC-GSA-PSO	Hybrid Gravitational Search Algorithm-Particle Swarm Optimization With Time Varying Acceleration Coefficients
SDEGCM	Self-Adaptive Differential Evolution with Gaussian–Cauchy Mutation
FSRPSO	A combination of Firefly Algorithm and Self-Regulating Particle Swarm Optimization
CSO	Crisscross Optimization Algorithm
ISNS	Improved Social Network Search Algorithm
IMPOA	Improved Marine Predators Algorithm
HNTMACSO	Multi-Agent-Based Crisscross Algorithm with Hybrid Neighboring Topology

* Corresponding authors: swathipolasa1982@gmail.com; harisheee@anurag.edu.in

1 Introduction

In a CHP system, fuel is burned to produce electrical and thermal energy at the same time. Cogeneration is frequently used to describe Combined Heat and Power (CHP) technology. CHP combined-cycle power plants may produce electricity and usable heat energy simultaneously from the same fuel. Thermal energy captured in the form of steam or hot water may be used for heating and cooling purposes as well as to generate power for various applications. Gas Turbines (GT), steam Turbines (ST), Reciprocating Engines (RE), Fuel Cells (FC), and MicroTurbines (MT) are the five main technologies used in CHP systems [1]. Industrial CHP is more appealing now that there is a greater emphasis on sustainability since it has a lower carbon footprint than on-site fuel burning, steam generation, and grid electricity import. CHP might be economically advantageous in green homes, wastewater treatment facilities, hospitals, data centers, various material processing plants, and so on. The most common objective function model is the reduction of overall production costs. The CHPED problem is an optimization problem that tends to reduce the generation cost of the CHP system. Because it directly affects power system efficiency, cost-effectiveness, and the sustainability of energy production, CHPED is an important goal. CHPED increases grid and system reliability, improves environmental goals and regulatory compliance, and maximizes overall efficiency. Since the early 1990s, numerous studies have used computer programming and mathematical methods to solve the economic dispatch problem for CHP systems. The CHPED problem becomes a nonconvex optimization problem because of the valve point effect of the thermal power plant. Also, including a prohibited operating zone for the thermal power plant and a feasible operating zone for the cogeneration plant transforms the CHPED problem into a complex, nonlinear, nonconvex, non-smooth optimization problem. Different methods used to solve the CHPED problem are shown in Figure 1.

2 Literature review

For the CHPED problem, classical mathematical programming methods were presented in [2] and [3]. Dual, Partial-Separable programming was implemented in [2] in Fortran 77 language. Here, the CHP issue is divided into two levels involving the distribution of heat and power: the bottom level determines production levels based on provided multipliers, while the top level adapts these multipliers to ensure that power production matches the demand, the algorithm has slow convergence. In [3], A two-layered algorithm is proposed, and the CHP issue is divided into sub-problems related to the distribution of heat and power. The power dispatch problem is solved iteratively in the outer layer using the Lagrangian Relaxation approach. During each iteration, the inner layer solves the heat dispatch using the unit heat capacity provided by the outer layer. The two sub-problems are linked by the heat-power feasible operating region (FOR) limits of cogeneration units. However, the algorithm took a lot of time for each iteration. The direct solution was given to the CHPED problem in [4, 5]. In [4], the optimal marginal costs ($\lambda - s$) formula was utilized to compute the cost that corresponds to a given heat and power demand. In [5], an explicit formula has been created for calculating incremental costs for the ideal dispatch for the overall system. A study made in [6] offered a Linear Programming (LP) formulation with a unique structure and created a simplex algorithm that effectively makes use of this structure and is five times faster than simplex.

A deterministic network flow model using LP of a typical CHP system was made in [7], where a system $\lambda - s$ matching the required power and heat demands formula was constructed. The Network flow model has the benefit of making it easier to interpret the data because it is simple to visualize the thermal and electric energy flows through the CHP equipment. The work of the Two-stage mathematical programming approach for the solution of the CHPED problem was done in [8]. An equivalent Mixed-Integer Quadratically Constrained Quadratic Program (MIQCQP) problem is resolved in the first stage. The solution region in the FOR is identified using the findings from solving Problem I. In [9], a microgrid with an EV charging station, CHP generation, renewable energy resource, external power grid, and natural gas station was developed, satisfying both electricity and heat energy demand. They have formulated a long-term cost minimization problem and proposed a Lyapunov optimization-based approach for real-time energy management. In [10], an optimal dispatch model for an Integrated Energy System (IES) based on carbon trading and CHP with Power to Gas (P2G) and Carbon Capture System (CCS) is proposed. In the research work [11], the Filled Function Method (FFM) was used to address the CHPED optimization problem. Furthermore, the Taguchi approach is integrated with the FFM and a developed TFFM to determine the optimal initial parameters. The most significant advantage of the TFFM is that it always produces the same result for identical inputs, and all solutions are within the feasible range.

A study in [12] described CHPED problems as a Markov decision process (MDP), which makes the model well encapsulated to maintain the input and output features of diverse devices. MDP provides a mathematical framework for simulating decision-making in which outcomes are partly dictated by chance and partly under the decision-maker's control. This avoids complex linearization methods to manage non-smooth functions. An Enhanced Distributed Proximal Policy Optimization (EDPPO), which is an advanced deep reinforcement learning technique, is used to solve CHPED. In [13], a Deep Reinforcement Learning (DRL) based Crisscross Optimization (CSO) algorithm was mentioned. The purpose of adopting DRL is to decrease the number of dimensions and limit the range of the initial population in the CSO algorithm. Next, the Deep Deterministic Policy Gradient (DDPG) technique updated DRL by enabling quick decision-making to speed up CSO.

The method explained in [14] combined the Improved genetic algorithm and the multiplier updated in such a way that it has the advantage of automatically setting

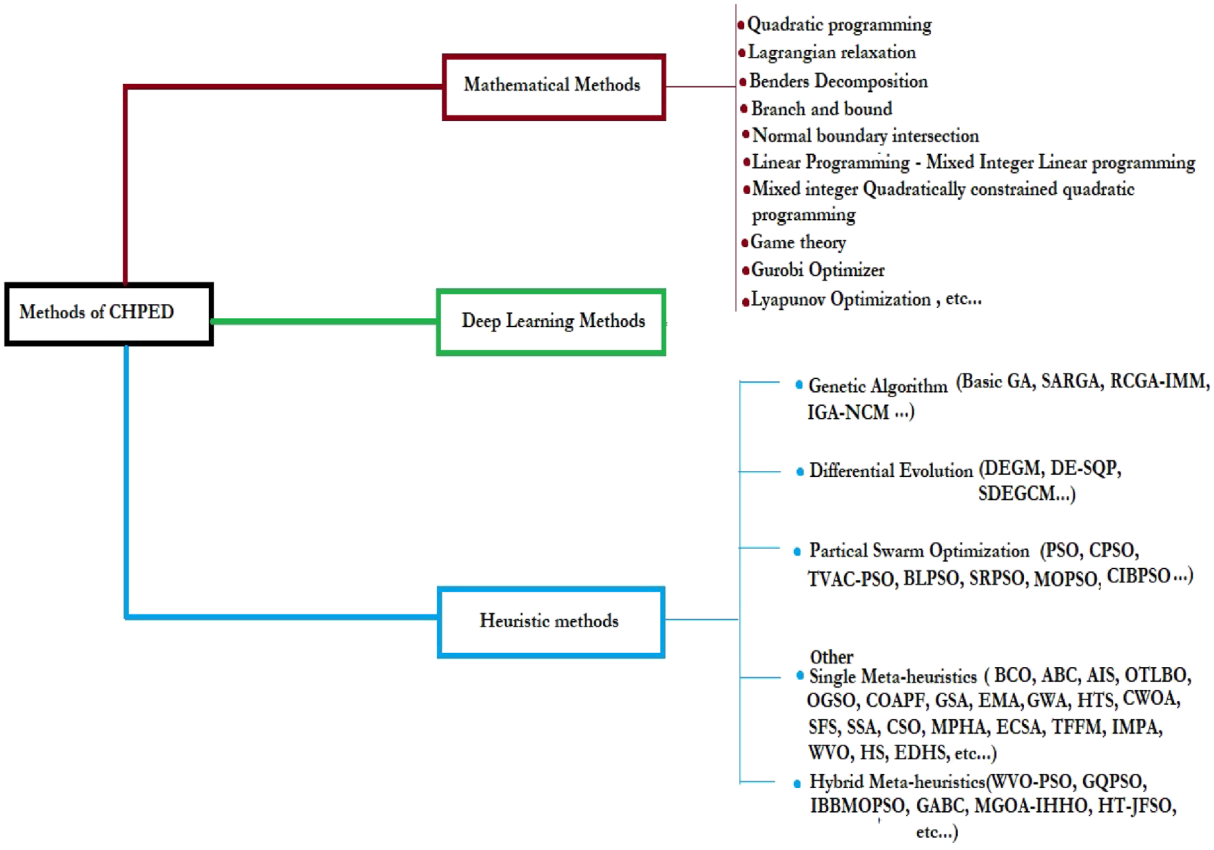

Figure 1. Different methods to solve CHPED problem.

the randomly assigned penalty to the appropriate value and only needs a modest population size for the CHPED issue. In [15], the CHPED problem was solved with a self-adaptive real-coded GA by considering the equality and inequality constraints simultaneously while integrating a penalty parameter-less constraint management approach. To produce superior offspring, the distribution index in the Simulated Binary Crossover (SBX) operator is used to introduce population variety. This results in a population with a high degree of variety, which can both improve the likelihood of reaching the global optimum and delay premature convergence. Real-coded GA with improved Muhlenbein mutation (RCGA-IMM) [16] is used to address the CHPED issue while taking the effect of valve-point loading and transmission losses into account. The Muhlenbein mutation is implemented in basic RCGA for speeding up the convergence and improving the optimization problem results. Two new Collective Information (CI)-based techniques, CI-based particle search, and CI-based elite fine-tuning, were developed in Collective Information-Based PSO (CIBPSO) [17]. IBBMOPSO studied in [18] integrates four improved strategies, namely: (i) a non-linear adaptive particle updating strategy is presented to automatically tune the weights of the personal (pbest) and the global (gbest) best positions respectively, and to reduce the standard deviation for generating new particles; (ii) an improved strategy by comparing the sparsity of the pbest and target particle to update pbest; (iii) To get the gbest for each target particle, a modified strategy that chooses a random Pareto optimal solution from a newly filtered subset of the external archive is used, and (iv) a new approach that combines the slope and the crowding distance is used. To enhance global search capabilities and avoid convergence to local minima, the research in [19] proposed combining the Continuous-Greedy Randomized Adaptive Search Process (C-GRASP) with DE and developed the C-GRASP-DE algorithm. Two strategies – Gaussian-Cauchy mutation and parameter self-adaptation – are used in Self-Adaptive DE with Gaussian-Cauchy mutation (SDEGCM) to enhance performance in [20]. Moreover, SDEGCM employed a constraint repair technique to address complicated operational restrictions. The suggested SDEGCM has provided better values in terms of solution stability and accuracy for the large-scale CHPED problem. Opposition-based GSO is presented in [21] and used to solve the CHPED issue by considering factors like VPE, Transmission loss, etc. The GSO algorithm in [22] used opposition-based learning for both population initialization and intelligent iteration updating. The core ranging mechanism of the Modified-GSO (MGSO) was presented in [22] to solve the CHPED problem on a large-scale test systems and prevent premature convergence is known as the B-Spline Wavelet (BW) theory. A One-Rank Cuckoo Search Algorithm (ORCSA) approach was developed and utilized in [23] to achieve the best possible solution quality and computational efficiency. In [24], a Grey wolf optimization technique is used to reduce costs while taking valve point influences and the CHP units' dual dependence on heat and electricity generation into account. The Harmony

Search approach is integrated with GA and developed HSGA [25] to obtain the solution of the CHPED problem. This algorithm uses a unique crossover operator. Basically, HS is used to ensure a high probability of assessing the global optimum by identifying inferior individuals. In [26], an improved HS method for addressing the CHPED problem is provided, in which the bandwidth adjustment is updated to obtain better results in terms of operational cost. In [27], a swarm-based algorithm inspired by honeybee food foraging behaviour is applied to the CHPED problem. It was observed that the algorithm delivered a better solution with less computational work. An optimization method called the Invasive Weed Optimization (IWO) algorithm is employed to solve the CHPED issue, which is based on the ecological process of weed colonization and dissemination [28]. In [29], an integration of Opposition-Based Learning (OBL) with Teaching Learning Based Optimization (TLBO) was employed to solve the CHPED problem in order to achieve less computational time and lower operational costs. A hybrid Firefly and Self-Regulating PSO (FSRPSO) method is used in [30] to address the CHPED problem. The FSRPSO leveraged the strengths of both the Firefly Algorithm (FA) and the SRPSO processes to balance the exploration and exploitation phases. The appropriate convergence speed and accuracy of the Crisscross optimization algorithm are better due to the use of the two stated crossover operators [31]. The vertical crossover operator is changed in [32] while tackling large-scale CHPED optimization problems, considering VPE, power transmission losses, and POZs of conventional thermal units. In [33], the Multi-Verse Optimization (MVO) method was developed, and it makes use of three astrophysical concepts: white holes, black holes, and wormholes, which are used to explore the evolution of the cosmos. An improved marine predators' optimization algorithm (IMPOA) was suggested in [34] for tackling the CHPED. In [35], a CSMO-Hybrid chameleon swarm algorithm and Mayfly optimization (MO) were proposed for tackling the CHPED issue that combines the Chameleon Swarm Algorithm (CSA) and MO. In [36], a powerful algorithm was designed by combining the Modified Grasshopper Optimization Algorithm (MGOA) and the improved Harris Hawks Optimizer (IHHO) in order to achieve a better balance between the early phases of global search and the latter stages of global convergence. MGOA-IHHO is the abbreviation for the proposed endeavor. The CHPED issue was investigated by combining a Strong Exploitation Strategy (SES) with a social network search (SNS) optimizer to produce an Improved SNS (ISNS) in [37] that improved SNS performance by boosting searching around the best view of all users. A metaheuristic method, Imperialist Competitive Harris Hawks Optimization [38], is used to address the Multi-Zone CHPED (MZCHPED) problem.

The application of classical methods is limited to solving CHPED issues under certain simplifying assumptions, which serve to make the optimization problem more manageable and less complex. Within deterministic models, it is assumed that the problem is free from both inherent and external disruptions and inaccuracies. This ideal assumption is invalid in practical implementations, and the differences can be significant under certain circumstances. Deep learning methods need improvement to be applicable to complex CHPED problems. Stochastic models are more commonly used for analyzing power dispatch problems because they can account for the presence of imprecise and unpredictable components that are typically present in system operation. Currently, numerous optimization methods that simulate different natural phenomena have been suggested and utilized to address this intricate challenge. These algorithms assert that they outperform similar optimization algorithms in terms of precision and execution time. According to the No Free Lunch Theorem [39], there is no metaheuristic strategy that guarantees the global optimal solution for the CHPED problem. Therefore, to further optimize costs within a reasonable execution time, a new algorithm was developed and used in the current research.

The main contributions of this paper are summarised as follows:

1. For the first time, a novel bio-inspired method called the LCA is introduced to address the medium and large-scale CHPED problems.
2. Random Opposition-Based Learning (ROBL) strategy is used to initialize the population. This strategy accelerates the search process and avoids getting stuck in a local optimum.
3. Valve-point loading effect is considered for power-only units.
4. The proposed method has been proven through extensive trials for solving the CHPED problem on four test systems, demonstrating its efficacy, efficiency, and superiority.

3 Problem formulation

A CHP system comprises power-only units that specifically generate electrical power, CHP units that concurrently generate power and heat, and heat-only units that generate heat specifically. This study aims to identify the most favourable outcomes while taking into account the limitations imposed by electricity consumption, power demand, heat demand, and other relevant factors.

The general optimization problem can be formulated as follows:

$$\text{Minimize } f(x, u), \tag{1}$$

$$\text{Subject to } g(x, u) = 0, \tag{2}$$

$$\text{and } h(x, u) \leq 0, \tag{3}$$

where, "f" is an objective function to be minimized. $g(x, u)$ represents the nonlinear equality constraints, such as real power and heat constraints. $h(x, u)$ represents the inequality constraints of the functional operating constraints, such as the Power limits of power-only units, the heat limits of heat-only units, and the feasible operating region of CHP units.

3.1. Objective Function:

Minimization of generation cost of CHP system: The aim of the CHP economic dispatch problem is to minimize the Cost of fuel, and is expressed as:

$$\text{Minimize } C = \sum_{i=1}^{N_p} C_{pi}(P_{pi}) + \sum_{j=1}^{N_c} C_{chpj}\left(P_{chpj}, T_{chpj}\right) + \sum_{k=1}^{N_h} C_{hk}(T_{hk}), \tag{4}$$

where C is the cost of overall production. P_{pi} is the power output, where pi is the power of ith power-only unit with valve point loading effect. P_{chpj} is the power output and T_{chpj} is the heat output, where $chpj$ is the jth CHP unit. T_{hk} is the heat output, where hk is the kth heat-only unit. C_{pi}, C_{chpj}, and C_{hk} are the unit costs when the output is P_{pi}, P_{chpj}, T_{chpj}, and T_{hk}, respectively C_{pi}, C_{chpj}, and C_{hk} are defined below:

$$C_{pi}(P_{pi}) = a_i P_{pi}^2 + b_i P_{pi} + c_i + |d_i \times \sin\left\{e_i\left(P_{pi}^{\min} - P_{pi}\right)\right\}|. \tag{5}$$

Typically, the fuel cost function for thermal power production units is represented by a quadratic function of active power outputs. Large power-producing units with steam turbines feature several steam admission valves. To obtain a continuously growing power output, these valves are opened one after the other. The valve opening results in throttling losses and wire pulling, which abruptly raises the heat rate. The presence of multiple valves in large steam turbine generators causes a phenomenon called the valve-point loading effect, which results in a rippling effect on the input-output characteristic [40]. The valve-point loading effect has been represented here by adding a sinusoidal term to the conventional cost function [41] and expressed in equation (5). Therefore, the output of the generation unit is not consistently stable, as depicted in Figure 2. Hence, the objective function is nonconvex. The cost functions of CHP units and heat-only units are expressed as follows:

$$C_{chpj}\left(P_{chpj}, T_{chpj}\right) = \alpha_j P_{chpj}^2 + \beta_j P_{chpj} + \gamma_j + \delta_j T_{chpj}^2 + \varepsilon_j T_{chpj} + \zeta_j P_{chpj} T_{chpj} \tag{6}$$

$$C_{hk}(T_{hk}) = \varphi_k + \eta_k T_{hk} + \lambda_k T_{hk}^2 \tag{7}$$

where a_i, b_i, c_i, d_i, and e_i are the cost coefficients of the ith power-only unit. $P_{pi}^{\min}$ is the minimum limit of the ith power-only unit. α_j, β_j, γ_j, δ_j, ε_j, and ζ_j are the cost coefficients of the jth CHP unit. φ_k, η_k, and λ_k are the cost coefficients of the kth heat-only unit.

3.2 Constraints

3.2.1 Equality constraints

The power and heat outputs must satisfy the corresponding demands for electricity and heat.

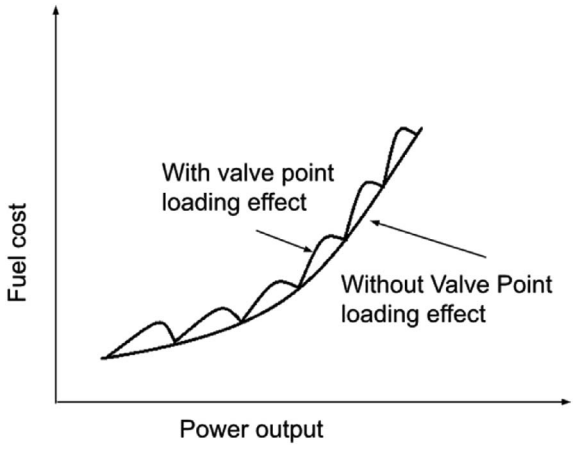

Figure 2. Cost curve of power units.

$$P_D = \sum_{i=1}^{N_p} P_{pi} + \sum_{j=1}^{N_c} P_{chpj}, \tag{8}$$

$$T_D = \sum_{j=1}^{N_c} T_{chpj} + \sum_{k=1}^{N_k} T_{hk}, \tag{9}$$

where P_D and T_D are the power demand and heat demand, respectively.

3.2.2 Inequality constraints

(a) Inequality constraints of power-only unit

The upper and lower bounds of the power-only unit's output can be represented as follows:

$$P_{pi}^{\min} \le P_{pi} \le P_{pi}^{\max}, \quad i \in 1, 2, \ldots N_P, \tag{10}$$

where $P_{pi}^{\min}$and $P_{pi}^{\max}$ are the lower and higher outputs of ith power-only unit, respectively.

(b) Inequality constraints of heat-only unit

The upper and lower bounds of the Heat-only unit's output can be represented as follows:

$$T_{hk}^{\min} \le T_{hk} \le T_{hk}^{\max}, \quad k \in 1, 2, \ldots N_h, \tag{11}$$

where $T_{hk}^{\min}$ and $T_{hk}^{\max}$ are the maximum and minimum outputs of k^{th} heat-only unit, respectively.

(c) Inequality constraints of the CHP unit

Power and heat generated by CHP units should be within the limits defined by the feasible operating region (FOR), as shown in Figure 3.

$$P_{chpj}^{\min}\left(T_{chpj}\right) \le P_{chpj} \le P_{chpj}^{\max}\left(T_{chpj}\right), \quad j \in 1, 2, \ldots N_c, \tag{12}$$

$$T_{chpj}^{\min}\left(P_{chpj}\right) \le T_{chpj} \le T_{chpj}^{\max}\left(P_{chpj}\right), \quad j \in 1, 2, \ldots N_c. \tag{13}$$

FOR is limited by (a) the generator's capacity-based maximum and minimum power output, which is the upper limit

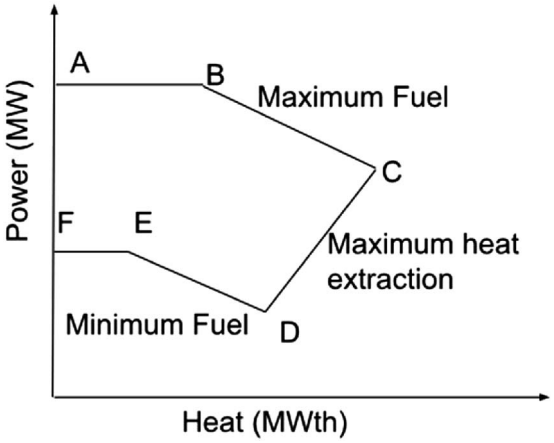

Figure 3. Feasible operating region of cogeneration plants.

for overloading risks and the lower limit for unstable operation; (b) the maximum and lower heat outputs, where low heat output indicates fuel waste and high heat output indicates exceeding design limits; and the addition of heat exchangers unit design, which limits the heat. (c) Since all steam is used for heating after power generation, the back-pressure line for the CHP unit's steam turbine specifies the high heat or low power limit; (d) the condensing line, which is important to the condensing turbine and is led by maximum power output, but reduces useful heat. (e) Iso-fuel curves, for constant fuel input.

4 Methodology to solve the CHPED problem by using the Liver Cancer algorithm

LCA is a novel biologically inspired technique introduced by Essam H. Houssein *et al.* in 2023 [42]. The behaviour of liver tumors serves as a source of inspiration for LCA and incorporates biological concepts into its optimization process. This makes it a unique and practical method for selecting features. Ten global optimization problems from the CEC'2020 test suite have been employed to evaluate the proposed LCA against several optimization algorithms, and from the results, it is concluded that the LCA has given better results in comparison to the other algorithms.

4.1 Liver cancer algorithm

The LCA algorithm is specifically developed to replicate the growth and dissemination patterns of liver tumors, which are cancerous growths in the liver that can significantly impair the body's functioning. The intricate nature of liver tumor growth, which involves interactions with the milieu and signalling pathways such as angiogenesis, immune evasion, and genetic alterations, serves as the motivation for the creation of LCA. Regarding optimization, the LCA algorithm imitates the pattern of expansion and dissemination of liver tumors within the liver. The algorithm's design is influenced by the adaptive nature of tumors, as they seek the most conducive environment for growth within the liver, as shown in Figure 4. The LCA technique comprises

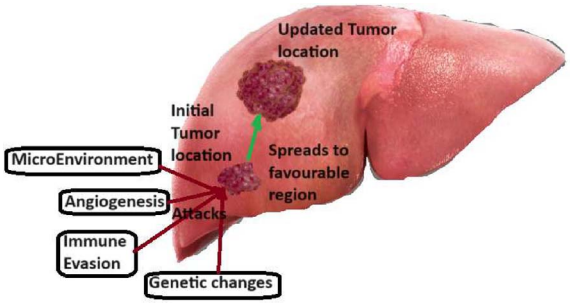

Figure 4. Tumor spread in liver.

multiple steps, each characterized by unique mathematical formulations, to accurately simulate the growth and behaviour of the tumour. The LCA algorithm uses ROBL to initialize the population. LCA employs variable approaches such as the jump strength method, Levy's flight function, and genetic operators during the exploitation phase, and this algorithm thoroughly explores the search space while striking a balance between local and global searches. The mutation rate is changed based on the number of iterations, and a higher mutation rate allows for the investigation of interesting new places while also preventing the algorithm from becoming stranded at a local minimum. As a result, a more optimal value can be obtained in less time. These features of LCA mentioned above make the LCA better than other contemporary algorithms mentioned in this work.

4.1.1 Tumor size calculation

The LCA algorithm [42] relies on the estimation of the tumor's size, which is crucial for the succeeding steps. A mathematical model was utilized to assess the size of the tumor. This model is based on the assumption that tumors have a hemi-ellipsoid shape, as shown in Figure 5, which has been found in other types of malignancies, including liver cancer [43]. The tumor is characterized by three dimensions: width, length, and height. Nevertheless, directly measuring the height dimension poses difficulties and is approximated via a mathematical model.

The size and position of the first tumor are determined using equation (14), which uses ROBL to create a starting population with a wide range of search exploration abilities.

$$\text{Position}_i^{*j} = \frac{\pi}{6} \cdot (\text{length}^j) \cdot \left(\text{width}^j\right) \cdot (\text{heightj}) - lb + (ub - lb) - rd * \text{Position}_i^j) \quad (14)$$

where $i = 1, 2, \ldots N$ and $j = 1, 2, \ldots D$. lb and ub represent the lower and upper boundaries of the decision variables, respectively. D is the dimension of the search area. The current position is Position_i, and the opposite position is Position_i^*. rd is a random number between 0 and 1. This random number is used to establish the initial population. The tumor position's size is determined by calculating the length of its diameters, which include width, height, and length, as shown in equation (15). The values for width

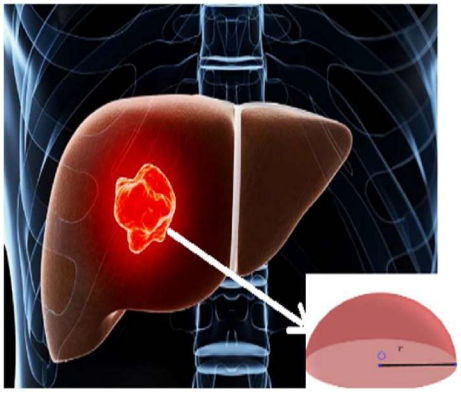

Figure 5. Shape of tumor.

and height are randomly generated numbers between 0 and 1.

$$\text{Position or tumor size } \frac{\pi}{6} \cdot f \cdot (l \cdot\ w)^{3/2} \tag{15}$$

where f, a constant equal to 1 for a specific type of tumor [44].

4.1.2 Tumor replication

The updating of tumor location is made based on different stages of cancer. The stage is defined by tumor position and size.

Stage I: If the tumor size is small, the tumor location is updated by the perch based on other family members or on a random tall tree. The increase in tumor position size (position) is calculated by equation (15).

Stage II: If the tumor size is increased and pushed to surrounding tissues, the tumor location is updated by the random jump strength of the tumor (Y) as shown in equation (17). Tumors replicate themselves in another place in the same liver organ in this stage.

$$(PG)^i = \frac{\mathrm{d}\,V}{\mathrm{d}t} = r * \text{ Position } t \in [1 \ldots T] \quad \text{and} \quad i \in [1 \ldots N], \tag{16}$$

$$\text{Updated position is } Y = \text{Position} + PG. \tag{17}$$

Stage III: If the tumor size is increased or multiple tumors are formed regionally, the tumor location is updated by the best way out of two methods: 1. Jump strength (Y), and 2. Based on Levy's flight function (Z) as shown in equation (22), this gives the best dive into the liver portions to capture them in competitive situations. Spread is increased to obtain a location where control of spread is minimal.

$$Z = Y + S \times Lv(D), \tag{18}$$

where S is a random number between 0 and 1,

$$Lv(D) = 0.01 \times \frac{\text{rand}(1, D) \times \sigma}{|\text{rand}(1, D)|^{1/\beta}}, \tag{19}$$

where D is the dimension of variables to be generated,

$$\sigma = \left[\left(\frac{\Gamma(1+\beta) \times \sin(\frac{\pi\beta}{2})}{\Gamma(\frac{1+\beta}{2}) \times \beta \times (2)^{(\frac{\beta-1}{2})}} \right) \right]^{1/\beta}, \tag{20}$$

where $\beta = 1.5$ and

$$\Gamma(x) = \int_0^\infty t^{(x-1)}\, e^{(-t)}\, \mathrm{d}t, \tag{21}$$

$$\text{Position}_{t+1}^i = \begin{cases} Y \text{ if fit}(Y) < \text{fit}(\text{Position}_t^i) \\ Z \textit{ if } \text{fit}(Z) < \text{fit}(\text{Position}_t^i) \end{cases}. \tag{22}$$

4.1.3 Tumor spreading using crossover and mutation

The final phase of the LCA algorithm signifies the advancement of a tumor to metastatic liver cancer, a sophisticated manifestation of the illness that originates in the liver but disseminates to additional regions of the body [45]. The LCA algorithm utilizes genetic operators, such as mutation and crossover, to provide extra variety in order to achieve its objective.

Stage IV: If the tumor size is spread to other organs, the tumor location is updated by a genetic algorithm that picks the best of three ways: mutated Y, mutated Z, and Crossover as shown in equation (27).

$$y_{\text{Mut}} = \begin{cases} \text{Position if} & \text{rand } 1 \geq \zeta \\ y & \text{else} \end{cases} \tag{23}$$

$$z_{\text{Mut}} = \begin{cases} \textit{Position} \text{ if} & \text{rand } 2 \geq \zeta \\ z & \text{else} \end{cases} \tag{24}$$

$$\text{Where} \begin{cases} \zeta = \dfrac{1}{T}; \\ y = |\text{Position} - \text{Position}_i^j|; \\ z = y - S \end{cases} \tag{25}$$

$$W_{\text{cross}} = \tau * y_{\text{Mut}} + (1 - \tau^{'}) * z_{\text{Mut}}, \quad \tau \neq \tau' \text{ random values } [0, 1] \tag{26}$$

$$\text{Position}_{t+1}^i = \begin{cases} y_{\text{Mut}} \textit{ if } \text{fit}(Y_{\text{Mut}}) < \text{fit}(\text{Position}_t^i) \\ z_{\text{Mut}} \textit{ if } \text{fit}(Z_{\text{Mut}}) < \text{fit}(\text{Position}_t^i) \\ W_{\text{cross}} \textit{ if } \text{fit}(W_{\text{cross}}) < \text{fit}(\text{Position}_t^i) \end{cases} \tag{27}$$

Pseudocode of Liver Cancer algorithm

1: Initialization: Initialize the population of liver tumor positions/locations by equation (14).
2: while (The termination requirement has not been satisfied) do
3: Estimate the tumor position fitness value. ⊳ Exploitation phase
4: if (Position < limit1), then
5: Update the tumor position with equation (15)
6: end if
7: else if (Position >= limit1) and (Position < limit2)
8: Update the tumor position by equation (17)
9: else if (Position >= limit2) and (Position < limit3)
10: Using equation (22), modify the position replication of the current search agent.
11: else Apply genetic operator equations (23)–(26) to calculate Position tumor spreading.
12: Using equation (27), update the current search agent's tumor position replication.
13: Validate and adjust the tumor positions to satisfy the constraints
13: Compute each tumor position fitness and search for best. ⊳ Exploration phase
14: $t = t + 1$
15: end while
16: Return best Fitness, Position

4.2 LCA in CHPED

N is the population size. Number of dimensions D that depicts Tumor location elements is $l_1 + l_{c1} + l_{h1}$, where $l_1 = N_p - 1$, $l_{c1} = N_c$, $l_{h1} = N_h - 1$, excluding slack power and slack heat units for power-only and heat-only units, respectively. The initialization of the population for X is given as equation (28).

$$X = \begin{bmatrix} X^1 \\ \cdot \\ \cdot \\ \cdot \\ X^i \\ \cdot \\ \cdot \\ \cdot \\ \cdot \\ X^N \end{bmatrix} = \begin{bmatrix} X_1^1, \ldots X_{Np-1}^1, \ldots & X_{Np-1+Nc}^1, \ldots & X_{Np-1+Nc+Nh-1}^1 \\ \cdot & & \cdot \\ \cdot & & \cdot \\ \cdot & & \cdot \\ X_1^i, \ldots X_{Np-1}^i, \ldots & X_{Np-1+Nc}^i, \ldots & X_{Np-1+Nc+Nh-1}^i \\ \cdot & & \cdot \\ \cdot & & \cdot \\ \cdot & & \cdot \\ \cdot & & \cdot \\ X_1^N, \ldots X_{Np-1}^N, \ldots & X_{Np-1+Nc}^N, \ldots & X_{Np-1+Nc+Nh-1}^N \end{bmatrix}. \tag{28}$$

The initial population is initialized using the ROBL technique (first generation data), satisfying inequality constraints of power-only units, heat-only units, and Cogeneration units. Fitness values, C for economic dispatch, are calculated using equation (4). The initial population of tumor location includes $N_p - 1$ power-only units, $N_h - 1$ heat-only units, N_c cogeneration plants, and excludes the slack power-only unit and the slack heat-only unit.

4.2.1 Constraints handling mechanism

The initialized population is populated in such a manner that it meets the inequality constraints of all Power-only except slack power-only unit, all Heat-only plants except for the slack heat-only unit, and all CHP plants. Slack power and slack heat are calculated to fulfill the power and heat demands using equations (29) and (30). Thus, equality and inequality constraints are met except for the inequality constraints of the slack power-only unit and the slack heat-only unit. The values of slack power and slack heat obtained are validated for capacity limits.

$$P_{\text{slack}} = P_D - \sum_{i=2}^{N_p} P_{pi} - \sum_{j=1}^{N_c} P_{chpj}, \tag{29}$$

$$T_{\text{slack}} = T_D - \sum_{k=2}^{N_h} T_{hk} - \sum_{j=1}^{N_c} T_{chpj}, \tag{30}$$

$$\text{Penalty}\, P_{\text{slack}} = \text{PenaltyFactor} * (P_{\text{slack}} - P_{\text{pslack}}^{\max}) \quad \text{if } P_{\text{slack}} > P_{\text{pslack}}^{\max}, \tag{31}$$

$$\text{Penalty}\, P_{\text{slack}} = \text{PenaltyFactor} * (P_{\text{pslack}}^{\min} - P_{\text{slack}}) \quad \text{if } P_{\text{slack}} < P_{\text{pslack}}^{\min}, \tag{32}$$

$$\text{Penalty}\, T_{\text{slack}} = \text{PenaltyFactor} * (T_{\text{slack}} - T_{\text{hslack}}^{\max}) \quad \text{if } T_{\text{slack}} > T_{\text{hslack}}^{\max}, \tag{33}$$

$$\text{Penalty}\, T_{\text{slack}} = \text{PenaltyFactor} * (T_{\text{hslack}}^{\min} - T_{\text{slack}}) \quad \text{if } T_{\text{slack}} < T_{\text{hslack}}^{\min}. \tag{34}$$

If they do not satisfy inequality constraints, penalty for power and penalty for heat are calculated by taking a very large penalty factor [46, 47] accordingly, as shown in equations (31)–(34). The total penalty is the sum of the power penalty and the heat penalty. Penalty is included in the objective function C. The LCA Algorithm will try to minimize the objective function C, and this can occur when the penalty is zero.

In each iteration, the best of fitness values (local best) calculated so far is assigned to Tumor Energy, and the corresponding data is assigned to Tumor location. In each iteration, the tumor size is calculated. Depending on tumor size (stage of Liver Cancer), next-generation data is updated one by one in the population. The fitness value of the next generation is calculated. If this value is less than the earlier (local best) value, then the Fitness value is assigned to Tumor Energy, and that data is assigned to Tumor location. This is looped until the total number of iterations is reached, as shown in the flow chart.

4.2.2 Flow chart

The flow chart is showcased in Figure 6.

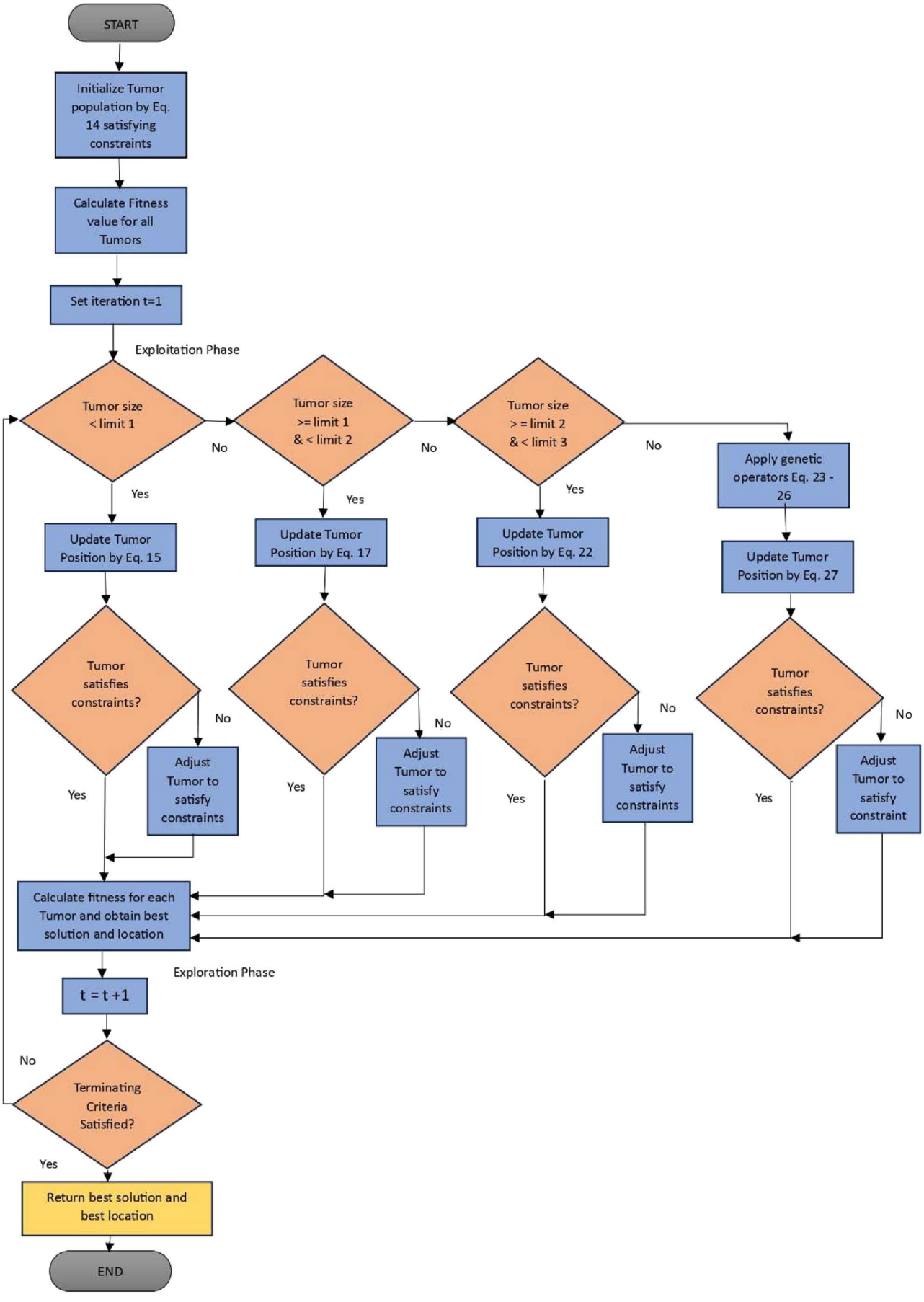

Figure 6. Flow chart of LCA applied to solve CHPED problem.

4.3 Simulation results and discussion

In order to showcase the efficiency and resilience of the suggested algorithm, it is applied to CHP systems with 48 units, 96 units, and 192 units. The simulation programs were implemented on a PC having Intel Core i5, 3.20 GHz, and 16GB RAM in MATLAB 2013a environment. All three test cases include the valve point loading effects for the power-only units. The LCA algorithm is run for 200 iterations with a population size of 60 for all the test cases. The parameter limits are 0.8 and 1.96 as indicated in [42]. After executing the program for a number of trials using different values for the parameters, it is observed that the parameter values shown in Table 1 are the best possible values that yielded better results. Hence, the parameters are set to the values shown in Table 1.

Table 1. The parameter setting of the proposed method.

Algorithm parameter	Numerical value
Limit 1	0.05
Limit 2	0.10
Limit 3	0.16

4.3.1 Testcase 1

In testcase 1, there are 26 power-only units, 12 CHP units, and 10 heat-only units, so the total units is 48. The data taken from [48] for the 48-unit system is shown in Table 2. The power limits for all power-only units, heat limits for all heat-only units, and the feasible operating region (FOR) for all CHP units are mentioned in Table 2. Units from P1 to P26 are 26 power-only units. Units from C1 to C12 are 12 CHP units. Units from H1 to H10 are 10 heat-only units. The power demand is 4700 MW, and the heat demand is 2500 MWth. To find the optimal performance of the LCA algorithm, the parameters are set to the values shown in Table 1. The convergence curve of case 48 using LCA is shown in Figure 7. From this figure, it is observed that the value of the penalty is zero from the first iteration onwards, and this depicts the efficiency of the algorithm in populating the values satisfying the constraints. Radar charts shown in Figures 8 and 9 support validating that the powers and heats generated by all the units satisfy the inequality constraints. The orange, blue, and red color charts in Figures 8 and 9 indicate the maximum, minimum, and actual values of all 26 power-only units and 10 heat-only units, respectively. From these figures, it is clear that the powers and heats generated are within the minimum and maximum limits for all power-only and heat-only units. To verify the satisfaction of constraints for the CHP system, line charts are utilized. Figures 10a–10d verify if the generations of cogeneration plants are within the feasible operating regions. C1 (HC1, PC1) is a point referring to the cogeneration plant C1 that generates heat HC1 and power PC1. All 12 cogeneration plants are highlighted in Figures 10a–10d. It can be seen that all cogeneration plants generate power and heat within FORs. Hence, all the inequality constraints are satisfied. For verification of power equality constraints, the powers generated by all power-only units and CHP units were added, and the result obtained was 4700 MW, which is the same as the total power demand. In similar lines, for the heat equality constraint, the heat produced by all CHP units and all heat-only units was added, and the sum obtained was 2500 MWth, which satisfies the heat demand. Hence, equality restrictions are also satisfied. The results for testcase 1 obtained by the LCA are compared with TVAC-PSO, OTLBO, TVAC-GSA-PSO, SDEGCM, DRL-CSO, and FSRPSO and are exhibited in Table 3. It is shown that the LCA technique gives the minimum best cost for case 48 of 113,616.5734 $/h (Dollar per hour) as compared to other techniques. The proposed LCA demonstrates convergence to the optimal value, ensuring the efficiency and reliability of the recommended technique, and achieves a superior solution of higher quality within reasonably fewer iterations when compared to the other algorithms mentioned.

4.3.2 Testcase 2

To verify the effectiveness of the proposed algorithm, it is implemented and tested for a larger-scale 96-unit CHP system. In 96-unit CHP system, there are 52 power-only units, 24 CHP units, and 20 heat-only units. Test data for 96 units is indicated in [51]. Units from P1 to P52 are 52 power-only units. Units from C1 to C24 are 24 CHP units. Units from H1 to H20 are 20 heat-only units. The power demand is 9400 MW, and the heat demand is 5000 MWth. To observe the better performance of the LCA algorithm, the parameters are set to the values shown in Table 1. The orange, blue, and red colors in Figures 11 and 12 indicate the maximum, minimum, and actual values of the powers and heats generated. Radar charts clearly show that the powers and heats generated are within the minimum and maximum limits for all power-only and heat-only units. All 24 cogeneration plants are highlighted in Figures 13a–13d. It can be seen that all the cogeneration plants generate power and heat within FORs. Hence, all the inequality constraints are met for testcase 2. Equality constraints are also satisfied. The details of the results using LCA are shown in Table 4. Comparison of the results of the best cost of the proposed algorithm is made with other algorithms like CSO, ISNS, SADEGCM, IMPOA, and DRL-CSO in Table 5. It can be seen that the proposed algorithm outperforms all other algorithms for testcase 2. The minimum cost of LCA is 220,107.797 $/h, whereas the other algorithms are in the range of 233,326.532 $/h. Nearly 13000 $/h amount is saved using the proposed algorithm LCA. It is evident that the LCA is a more effective algorithm in solving CHPED problems.

Table 2. Cost function of all units of Testcase 1.

Unit No.	Cost function (Eqs. (5)–(7))	Capacity Limits (MW/MWth)/ FOR number
P1	$C_1(P_{1)} = 0.00028\ P_1^2 + 8.1P_1 + 550 + \lvert 300\ \sin(0.035 \times (-P_1))\rvert$	$0 \le P_1 \le 680$
P2	$C_2(P_2) = 0.00056\ P_2^2 + 8.1P_2 + 309 + \lvert 200\ \sin(0.042 \times (-P_2))\rvert$	$0 \le P_2 \le 360$
P3	$C_3(P_3) = 0.00056\ P_3^2 + 8.1P_3 + 309 + \lvert 200\ \sin(0.042 \times (-P_3))\rvert$	$0 \le P_3 \le 360$
P4	$C_4(P_4) = 0.00324\ P_4^2 + 7.74P_4 + 240 + \lvert 150\ \sin(0.063 \times (60 - P_4))\rvert$	$60 \le P_4 \le 180$
P5	$C_5(P_5) = 0.00324\ P_5^2 + 7.74P_5 + 240 + \lvert 150\ \sin(0.063 \times (60 - P_5))\rvert$	$60 \le P_5 \le 180$
P6	$C_6(P_6) = 0.00324\ P_6^2 + 7.74P_6 + 240 + \lvert 150\ \sin(0.063 \times (60 - P_6))\rvert$	$60 \le P_6 \le 180$
P7	$C_7(P_7) = 0.00324\ P_7^2 + 7.74P_7 + 240 + \lvert 150\ \sin(0.063 \times (60 - P_7))\rvert$	$60 \le P_7 \le 180$
P8	$C_8(P_8) = 0.00324\ P_8^2 + 7.74P_8 + 240 + \lvert 150\ \sin(0.063 \times (60 - P_8))\rvert$	$60 \le P_8 \le 180$
P9	$C_9(P_9) = 0.00324\ P_9^2 + 7.74\ P_9 + 240 + \lvert 150\ \sin(0.063 \times (60 - P_9))\rvert$	$60 \le P_9 \le 180$
P10	$C_{10}(P_{10}) = 0.00284\ P_{10}^2 + 8.6\ P_{10} + 126 + \lvert 100\ \sin(0.084 \times (40 - P_{10}))\rvert$	$40 \le P_{10} \le 120$
P11	$C_{11}(P_{11}) = 0.00284\ P_{11}^2 + 8.6\ P_{11} + 126 + \lvert 100\ \sin(0.084 \times (40 - P_{11}))\rvert$	$40 \le P_{11} \le 120$
P12	$C_{12}(P_{12}) = 0.00284\ P_{12}^2 + 8.6\ P_{12} + 126 + \lvert 100\ \sin(0.084 \times (55 - P_{12}))\rvert$	$55 \le P_{12} \le 120$
P13	$C_{13}(P_{13}) = 0.00284\ P_{13}^2 + 8.6\ P_{13} + 126 + \lvert 100\ \sin(0.084 \times (55 - P_{13}))\rvert$	$55 \le P_{13} \le 120$
P14	$C_{14}(P_{14}) = 0.00028\ P_{14}^2 + 8.1\ P_{14} + 550 + \lvert 300\ \sin(0.035 \times (-P_{14}))\rvert$	$0 \le P_{14} \le 680$
P15	$C_{15}(P_{15}) = 0.00056\ P_{15}^2 + 8.1P_{15} + 309 + \lvert 200\ \sin(0.042 \times (-P_{15}))\rvert$	$0 \le P_{15} \le 360$
P16	$C_{16}(P_{16}) = 0.00056\ P_{16}^2 + 8.1\ P_{16} + 309 + \lvert 200\ \sin(0.042 \times (-P_{16}))\rvert$	$0 \le P_{16} \le 360$
P17	$C_{17}(P_{17}) = 0.00324\ P_{17}^2 + 7.74\ P_{17} + 240 + \lvert 150\ \sin(0.063 \times (60 - P_{17}))\rvert$	$60 \le P_{17} \le 180$
P18	$C_{18}(P_{18}) = 0.00324\ P_{18}^2 + 7.74\ P_{18} + 240 + \lvert 150\ \sin(0.063 \times (60 - P_{18}))\rvert$	$60 \le P_{18} \le 180$
P19	$C_{19}(P_{19}) = 0.00324\ P_{19}^2 + 7.74\ P_{19} + 240 + \lvert 150\ \sin(0.063 \times (60 - P_{19}))\rvert$	$60 \le P_{19} \le 180$
P20	$C_{20}(P_{20}) = 0.00324\ P_{20}^2 + 7.74\ P_{20} + 240 + \lvert 150\ \sin(0.063 \times (60 - P_{20}))\rvert$	$60 \le P_{20} \le 180$
P21	$C_{21}(P_{21}) = 0.00324\ P_{21}^2 + 7.74\ P_{21} + 240 + \lvert 150\ \sin(0.063 \times (60 - P_{21}))\rvert$	$60 \le P_{21} \le 180$
P22	$C_{22}(P_{22}) = 0.00324\ P_{22}^2 + 7.74\ P_{22} + 240 + \lvert 150\ \sin(0.063 \times (60 - P_{22}))\rvert$	$60 \le P_{22} \le 180$
P23	$C_{23}(P_{23}) = 0.00284\ P_{23}^2 + 8.6\ P_{23} + 126 + \lvert 100\ \sin(0.084 \times (40 - P_{23}))\rvert$	$40 \le P_{23} \le 120$
P24	$C_{24}(P_{24}) = 0.00284\ P_{24}^2 + 8.6\ P_{24} + 126 + \lvert 100\ \sin(0.084 \times (40 - P_{24}))\rvert$	$40 \le P_{24} \le 120$
P25	$C_{25}(P_{25}) = 0.00284\ P_{25}^2 + 8.6\ P_{25} + 126 + \lvert 100\ \sin(0.084 \times (55 - P_{25}))$	$55 \le P_{25} \le 120$
P26	$C_{26}(P_{26}) = 0.00284\ P_{26}^2 + 8.6\ P_{26} + 126 + \lvert 100\ \sin(0.084 \times (55 - P_{26}))$	$55 \le P_{26} \le 120$
C1	$C_{27}(P_{27}, H_{27}) = 0.0345\ P_{27}^2 + 14.5\ P_{27} + 0.03\ H_{27}^2 + 4.2\ H_{27} + 0.031\ P_{27}\ H_{27} + 2650$	#1
C2	$C_{28}(P_{28}, H_{28}) = 0.0435\ P_{26}P_{28}^2 + 36\ P_{28} + 0.027\ H_{28}^2 + 0.6\ H_{28} + 0.011\ P_{28}\ H_{28} + 1250$	#2
C3	$C_{29}(P_{29}, H_{29}) = 0.0345\ P_{29}^2 + 14.5\ P_{29} + 0.03\ H_{29}^2 + 4.2\ H_{29} + 0.031\ P_{29}\ H_{29} + 2650$	#1
C4	$C_{30}(P_{30}, H_{30}) = 0.0435\ P_{30}^2 + 36\ P_{30} + 0.027\ H_{30}^2 + 0.6\ H_{30} + 0.011\ P_{30}\ H_{30} + 1250$	#2
C5	$C_{31}(P_{31}, H_{31}) = 0.1035\ P_{31}^2 + 34.5\ P_{31} + 0.025\ H_{31}^2 + 2.203\ H_{31} + 0.051\ P_{31}\ H_{31} + 2650$	#3
C6	$C_{32}(P_{32}, H_{32}) = 0.072\ P_{32}^2 + 20\ P_{32} + 0.02\ H_{32}^2 + 2.34\ H_{32} + 0.04\ P_{32}\ H_{32} + 1565$	#4
C7	$C_{33}(P_{33}, H_{33}) = 0.0345\ P_{33}^2 + 14.5\ P_{33} + 0.03\ H_{33}^2 + 4.2\ H_{33} + 0.031\ P_{33}\ H_{33} + 2650$	#1
C8	$C_{34}(P_{34}, H_{34}) = 0.0435\ P_{34}^2 + 36\ P_{34} + 0.027\ H_{34}^2 + 0.6\ H_{34} + 0.011\ P_{34}\ H_{34} + 1250$	#2
C9	$C_{35}(P_{35}, H_{35}) = 0.0345\ P_{34}^2 + 14.5\ P_{35} + 0.03\ H_{35}^2 + 4.2\ H_{35} + 0.031\ P_{35}\ H_{35} + 2650$	#1
C10	$C_{36}(P_{36}, H_{36}) = 0.0435\ P_{36}^2 + 36\ P_{36} + 0.027\ H_{36}^2 + 0.6\ H_{36} + 0.011\ P_{36}\ H_{36} + 1250$	#2
C11	$C_{37}(P_{37}, H_{37}) = 0.1035\ P_{37}^2 + 34.5\ P_{37} + 0.025\ H_{37}^2 + 2.203\ H_{37} + 0.051\ P_{37}\ H_{37} + 2650$	#3
C12	$C_{38}(P_{38}, H_{38}) = 0.072\ P_{38}^2 + 20\ P_{38} + 0.02\ H_{38}^2 + 2.34\ H_{38} + 0.04\ P_{38}\ H_{38} + 1565$	#4
H1	$C_{39}(H_{39}) = 0.038\ H_{39}^2 + 2.0109\ H_{39} + 950$	$0 \le H_{39} \le 2695.2$
H2	$C_{40}(H_{40}) = 0.038\ H_{40}^2 + 2.0109\ H_{40} + 950$	$0 \le H_{40} \le 60$
H3	$C_{41}(H_{41}) = 0.038\ H_{41}^2 + 2.0109\ H_{41} + 950$	$0 \le H_{41} \le 60$
H4	$C_{42}(H_{42}) = 0.052\ H_{42}^2 + 3.0651\ H_{42} + 480$	$0 \le H_{42} \le 120$
H5	$C_{43}(H_{43}) = 0.052\ H_{43}^2 + 3.0651\ H_{43} + 480$	$0 \le H_{43} \le 120$
H6	$C_{44}(H_{44}) = 0.038\ H_{44}^2 + 2.0109\ H_{44} + 950$	$0 \le H_{44} \le 2695.2$
H7	$C_{45}(H_{45}) = 0.038\ H_{45}^2 + 2.0109\ H_{45} + 950$	$0 \le H_{45} \le 60$
H8	$C_{46}(H_{46}) = 0.038\ H_{46}^2 + 2.0109\ H_{46} + 950$	$0 \le H_{46} \le 60$
H9	$C_{47}(H_{47}) = 0.052\ H_{47}^2 + 3.0651\ H_{47} + 480$	$0 \le H_{47} \le 120$
H10	$C_{48}(H_{48}) = 0.052\ H_{48}^2 + 3.0651\ H_{48} + 480$	$0 \le H_{48} \le 120$

#1–#4 are FORs mentioned in Figures 10a–10d.

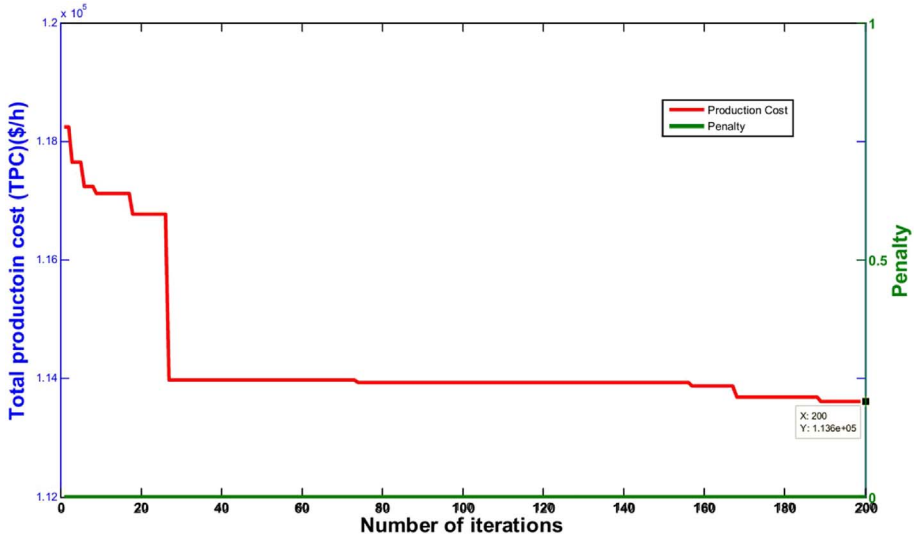

Figure 7. Convergence curve using LCA for Testcase 1.

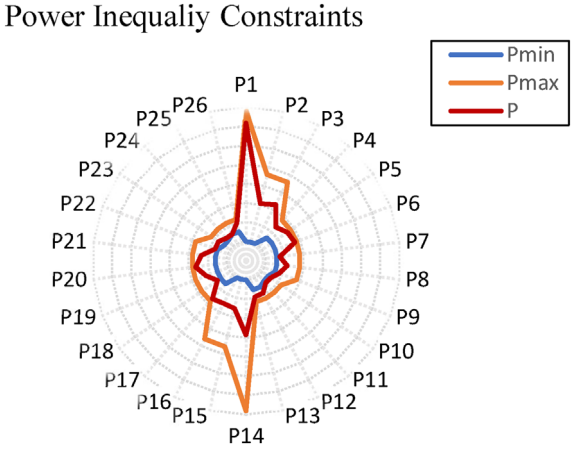

Figure 8. Power outputs of testcase 1.

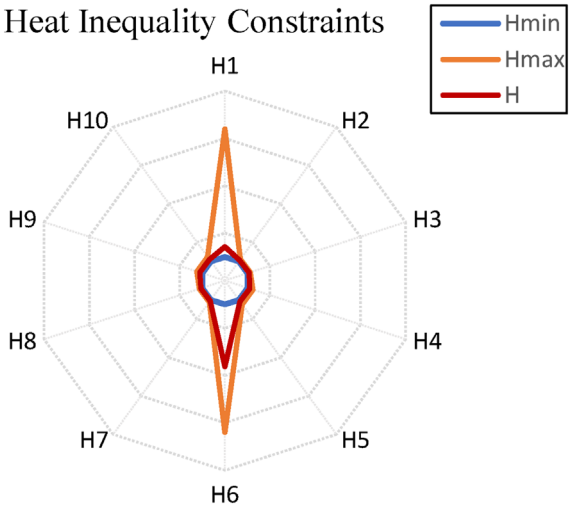

Figure 9. Heat outputs of testcase 1.

4.3.3 Testcase 3

Furthermore, to test the performance of the proposed algorithm LCA for very large scale, it is implemented for 192 units testcase 3. Testcase 3 includes 104 power-only units, 48 cogeneration units, and 20 heat-only units. Test data for 192 units is available in [13, 52, 53]. Units from P1 to P104 are 104 power-only units. Units from C1 to C48 are 48 number of CHP units. Units from H1 to H40 are 40 heat-only units. The power demand is 18,800 MW, and the heat demand is 10,000 MWth. To obtain a better performance of the LCA algorithm, the parameters are set to the values shown in Table 1. All the equality and inequality restrictions are met for testcase 3. The details of the results using LCA are shown in Table 6. The values of power are in MW and the heat in MWth. In Table 7, the results are compared to other methods such as CSO, NDIDE, HNTMACSO, and DRL-CSO. It is visible clearly that the LCA algorithm yields better results compared to others.

4.4 Statistical analysis of the performance of the Liver Cancer Algorithm

The statistical values described by minimum, maximum, average values, and standard deviation, along with the execution time obtained from 20 trials of different algorithms, including LCA for testcases 1, 2, and 3, are shown in Table 8. The execution time of LCA is less than that of TVAC-PSO, SDEGCM, DRL-CSO, and OTLBO algorithms for testcase 1. The costs are significantly less compared to all other algorithms for all the test cases taken in this paper.

It is also observed that the proposed algorithm gives the same optimal value most of the time when executed consecutively. The minimum value is obtained in nearly 80% of 20 trials for testcase 48 using LCA, as shown in Figure 14. Also, to appreciate the performance of the proposed algorithm, the Wilcoxon signed rank test is carried out. This

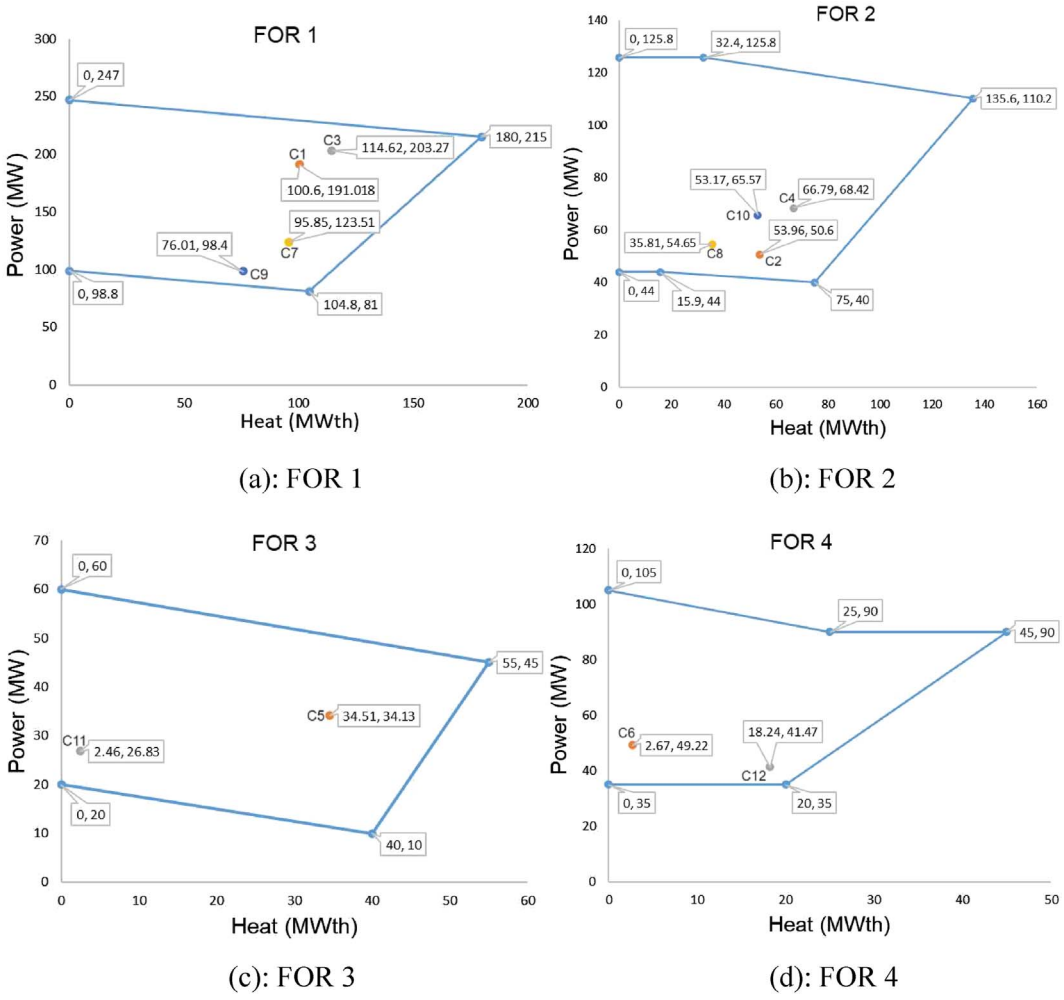

Figure 10. (a): FOR 1. (b): FOR 2; (c) FOR 3; (d) FOR 4.

Table 3. Comparison of LCA with other algorithms for Testcase 1.

Output	TVAC-PSO [49]	OTLBO [29]	TVAC-GSA-PSO [50]	SDEGCM [20]	DRL-CSO [13]	FSRPSO [30]	LCA
P1	538.5587	628.3199	448.8100	538.5588	521.7830	89.7600	615.8407
P2	75.1340	225.3313	149.6300	299.3135	299.2610	224.4000	205.0118
P3	75.1340	223.9653	299.2800	299.1953	225.6760	0.0000	229.1592
P4	140.6146	159.8516	110.0000	109.8697	159.7120	180.0000	131.0036
P5	140.6146	109.9150	109.8400	109.8677	159.7180	180.0000	160.7069
P6	140.6146	159.7795	60.0000	109.8675	159.6260	159.7300	171.3829
P7	140.6146	109.8946	160.1800	159.7333	159.6420	159.7300	75.4313
P8	140.6146	109.9321	60.0100	109.8670	109.4170	109.8700	113.8211
P9	140.6146	159.9569	159.9800	109.8666	110.0510	109.8700	83.4828
P10	112.1998	40.8970	114.5000	40.0065	40.2630	77.4000	54.2162
P11	112.1998	41.3115	78.1800	40.0000	40.0000	40.0000	53.4071
P12	74.7999	55.1748	92.0900	55.0000	55.6590	112.9700	89.3761
P13	74.7999	92.4003	92.4500	55.0013	55.3560	55.0000	94.0329
P14	269.2794	448.8359	359.0700	628.3188	447.7840	680.0000	284.9940

(Continued on next page)

Table 3. (Continued)

Output	TVAC-PSO [49]	OTLBO [29]	TVAC-GSA-PSO [50]	SDEGCM [20]	DRL-CSO [13]	FSRPSO [30]	LCA
P15	299.1993	225.7871	356.6500	299.4114	299.1610	299.2000	155.6874
P16	299.1993	75.4600	359.9900	299.2580	225.0760	360.0000	151.7351
P17	140.3973	160.1192	159.7400	109.8675	159.8120	109.8700	164.3305
P18	140.3973	110.3532	60.0100	109.8668	159.7770	159.7300	81.5633
P19	140.3973	159.8190	159.7200	109.8680	159.1330	159.7300	121.8521
P20	140.3973	159.7765	159.8000	109.8667	159.7220	109.8700	164.0053
P21	140.3973	159.7370	159.7100	109.8668	109.7620	159.7300	133.5927
P22	140.3973	160.1751	159.4600	109.8685	109.6120	109.8700	71.3839
P23	74.7998	40.1140	78.6900	40.0164	40.5320	77.4000	74.5984
P24	74.7998	40.3042	40.0000	40.0000	40.0000	114.8000	54.8435
P25	112.1997	92.4149	92.1900	55.0000	55.6590	55.0000	55.7440
P26	112.1997	92.5012	92.4600	55.0000	55.3560	92.4000	101.6974
PC1	86.9119	85.9857	114.1300	83.9905	81.5210	120.9400	191.0178
PC2	56.1027	98.3501	40.0000	40.0000	40.0000	66.0200	50.6059
PC3	86.9119	81.7197	81.0400	83.5598	81.6040	92.3300	203.2735
PC4	56.1027	48.9055	54.2500	40.0310	40.0000	54.9300	68.4209
PC5	10.0031	10.0832	10.0000	10.0106	10.0000	11.1000	34.1277
PC6	35.0000	39.3110	35.0500	35.0000	35.0000	53.9200	49.2195
PC7	95.4799	82.0236	86.6400	87.2893	84.6500	81.0000	123.5106
PC8	54.9235	40.1105	41.6400	40.3551	40.0000	55.3600	54.6546
PC9	95.4799	81.3039	86.1900	81.3165	84.6760	86.4400	98.4023
PC10	54.9235	45.6700	49.4800	40.0149	40.0000	40.0000	65.5681
PC11	23.4981	13.8709	10.0000	10.0000	10.0000	10.0000	26.8334
PC12	54.0882	30.3881	35.0000	36.0762	35.0000	41.6400	41.4657
HC1	108.1177	107.5951	123.3800	106.4783	104.7510	127.2200	100.6010
HC2	88.9006	125.4997	74.9800	75.0000	75.0000	97.4600	53.9614
HC3	108.1177	105.1942	104.8100	106.2365	104.5750	111.1600	114.6176
HC4	88.9006	82.6853	87.2800	75.0268	75.0000	87.8900	66.7871
HC5	40.0013	40.0346	40.0000	40.0045	40.0000	35.6000	34.5111
HC6	20.0000	21.9568	20.0200	20.0000	20.0000	28.6000	2.6862
HC7	112.9260	105.3622	107.9500	108.3295	106.6620	179.9400	95.8526
HC8	87.8827	75.0938	76.4000	75.3065	75.0000	88.2600	35.8097
HC9	112.9260	104.9667	107.7000	104.9776	106.8420	107.8500	76.0110
HC10	87.8827	79.8936	83.1600	75.0129	75.0000	75.0000	53.1674
HC11	45.7849	41.6554	40.0000	40.0000	40.0000	55.0000	2.4596
HC12	28.6765	17.9018	20.0000	20.4892	20.0000	23.0200	18.2363
H1	433.9113	445.0937	455.3500	466.5934	471.5730	402.1900	218.9337
H2	60.0000	59.9967	60.0000	60.0000	465.5980	60.0000	23.9165
H3	60.0000	59.9974	60.0000	60.0000	60.0000	60.0000	41.4727
H4	120.0000	119.8834	120.0000	120.0000	60.0000	116.4300	48.8133
H5	120.0000	119.5231	120.0000	120.0000	60.0000	119.9900	48.3054
H6	415.9741	428.7605	439.0800	466.5453	60.0000	364.7100	1309.0190
H7	60.0000	59.9957	60.0000	60.0000	120.0000	60.0000	25.2895
H8	60.0000	59.9638	60.0000	60.0000	120.0000	59.7000	25.2439
H9	119.9989	119.5025	120.0000	120.0000	120.0000	120.0000	53.8272
H10	119.9989	119.4440	119.9200	119.9994	120.0000	120.0000	50.4780
Minimum cost ($/h)	117,824.8956	116,579.2390	117,438.6000	115,626.3697	115,952.9040	115,769.6300	113,616.5734

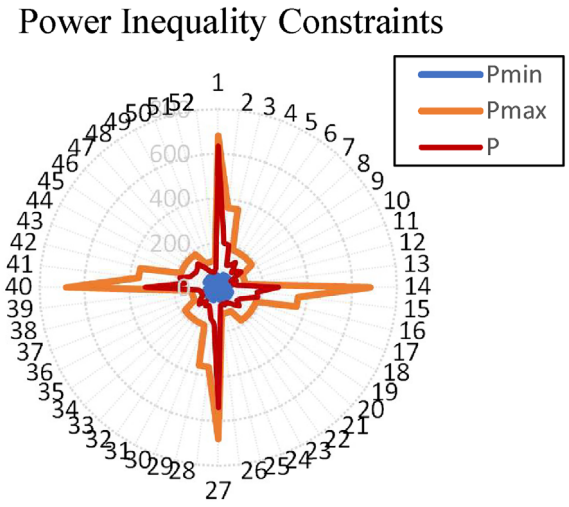

Figure 11. Power outputs of testcase 2.

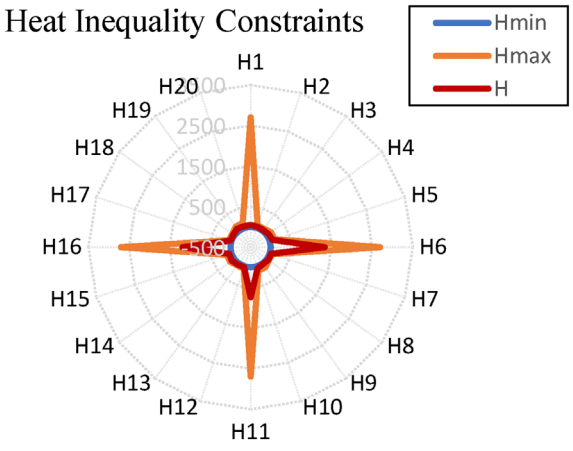

Figure 12. Heat outputs of testcase 2.

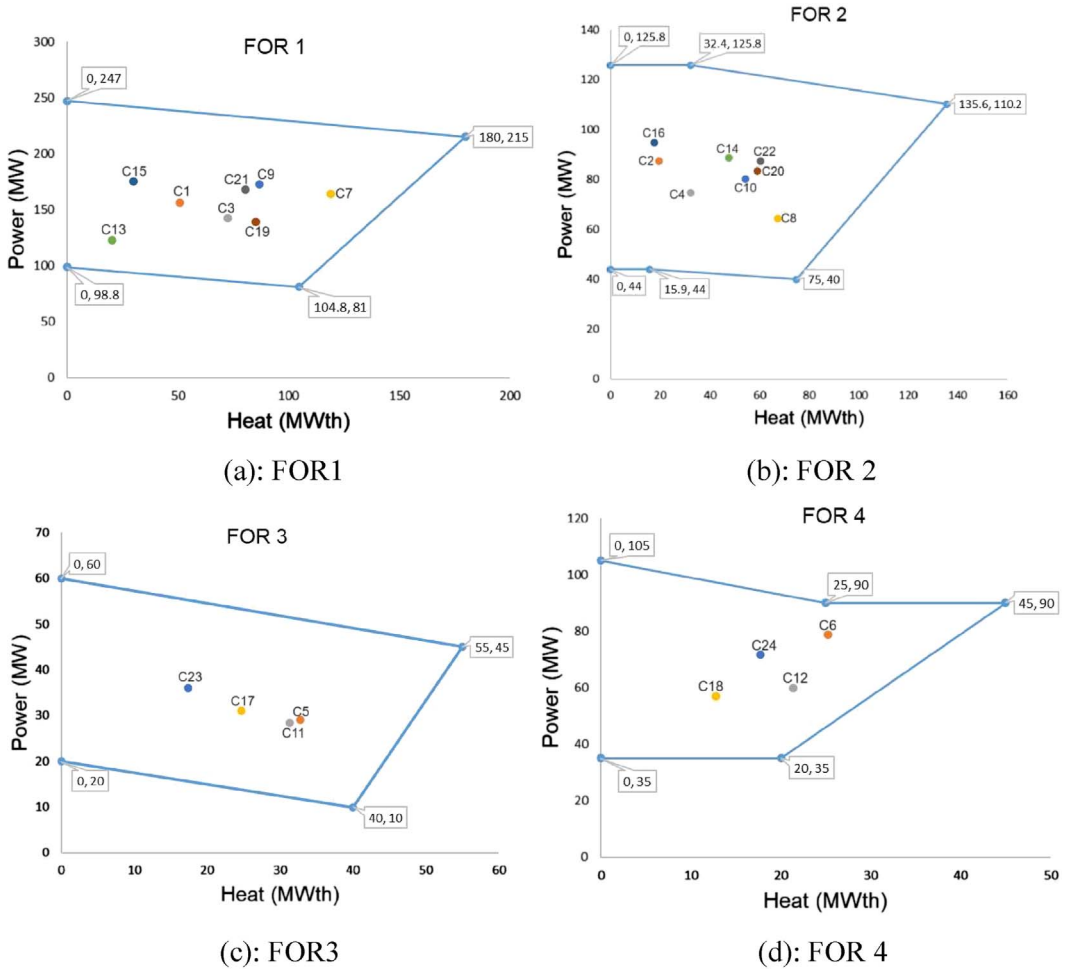

(a): FOR1 (b): FOR 2

(c): FOR3 (d): FOR 4

Figure 13. (a) FOR1; (b) FOR 2; (c) FOR3; (d) FOR 4.

Table 4. Power and heat outputs for Testcase 2 by using LCA.

Output	LCA	Output	LCA	Output	LCA	Output	LCA
P1	633.9052	P31	91.8152	PC9	172.3392	HC15	30.0187
P2	199.3129	P32	99.9317	PC10	80.3391	HC16	17.6110
P3	195.7011	P33	81.1341	PC11	28.4862	HC17	24.7040
P4	106.0671	P34	114.4249	PC12	59.8188	HC18	12.8020
P5	112.6452	P35	99.4784	PC13	122.6335	HC19	85.0419
P6	135.7901	P36	78.8779	PC14	88.7984	HC20	59.2587
P7	89.2933	P37	79.7016	PC15	175.1068	HC21	80.6028
P8	110.8289	P38	78.8720	PC16	94.7845	HC22	60.6187
P9	123.0948	P39	90.0729	PC17	31.0731	HC23	17.4061
P10	62.4198	P40	326.6076	PC18	56.8411	HC24	17.7183
P11	86.7591	P41	151.4736	PC19	139.1948	H1	45.8357
P12	66.8961	P42	178.5443	PC20	83.2924	H2	26.4607
P13	84.8416	P43	134.0330	PC21	168.0092	H3	25.5495
P14	269.1177	P44	127.6675	PC22	87.3473	H4	45.8108
P15	175.8122	P45	119.7915	PC23	36.0051	H5	63.2432
P16	181.9285	P46	125.7037	PC24	71.5751	H6	1324.9967
P17	134.4574	P47	139.7609	HC1	50.8147	H7	33.3306
P18	111.3028	P48	111.0229	HC2	19.6134	H8	33.5512
P19	101.1917	P49	83.2163	HC3	72.6182	H9	21.9557
P20	124.1047	P50	72.6660	HC4	32.2163	H10	50.6797
P21	104.0859	P51	71.4034	HC5	32.7384	H11	735.7315
P22	85.8164	P52	86.8316	HC6	25.2209	H12	21.8953
P23	77.5151	PC1	155.8835	HC7	119.0029	H13	30.4152
P24	83.8408	PC2	87.4471	HC8	67.3094	H14	73.3148
P25	76.6944	PC3	142.1985	HC9	86.9600	H15	56.4000
P26	81.0900	PC4	74.7368	HC10	54.4265	H16	1176.6354
P27	538.0677	PC5	29.1110	HC11	31.2930	H17	20.8150
P28	165.1890	PC6	78.6560	HC12	21.3489	H18	24.1935
P29	141.4577	PC7	164.2146	HC13	20.3405	H19	62.2662
P30	105.4413	PC8	64.4082	HC14	47.6604	H20	39.5734
						Minimum cost ($/h)	220,107.7978

Table 5. Comparison of LCA with other methods for Testcase 2.

Method	Minimum cost ($/h)
CSO [32]	233,663.273
ISNS [37]	233,543.659
SADEGCM [20]	231,590.4057
IMPOA [34]	235,260.3
DRL-CSO [13]	233,326.532
LCA	220,107.797

test is conducted at a significance level of 0.05, denoted as α. Statistical analysis provides the information regarding the acceptance or rejection of any hypothesis. Hypotheses can be evaluated by comparing statistical data with significance analysis, which determines whether to reject or retain them. If the statistical value is below the significance level, the hypothesis H_1 will be accepted; otherwise, it will be rejected. This indicates that the algorithm could minimize the cost to a greater extent, satisfying all the constraints. Table 9 displays the preservation of the hypothesis by the utilisation of the Wilcoxon signed-rank test.

Conclusion

This article presents a novel bio-inspired LCA as a demonstration of its effectiveness in addressing the CHPED problem for medium and large-scale systems. The proposed optimization methodology utilized a strong exploitative strategy, ROBL, to initialize the population, where searching is done throughout the search space and applied Levy's flight function, genetic operators to update the population in one iteration, and a precise exploration technique for searching the best solution. This approach generated

Table 6. Power and heat outputs for Testcase 3 by using LCA.

Output	LCA	Output	LCA	Output	LCA	Output	LCA
P1	656.666	P61	137.5071	PC17	37.12068	HC29	28.12447
P2	301.2447	P62	55.63833	PC18	55.76829	HC30	10.57424
P3	198.9702	P63	85.38637	PC19	111.3537	HC31	111.3371
P4	104.9259	P64	89.84113	PC20	98.95785	HC32	28.38863
P5	122.9232	P65	75.82256	PC21	193.9555	HC33	118.2612
P6	145.6228	P66	510.1585	PC22	64.23227	HC34	51.65592
P7	121.8947	P67	112.513	PC23	20.33282	HC35	31.61522
P8	160.8492	P68	74.32122	PC24	53.37086	HC36	2.631264
P9	110.6454	P69	101.1369	PC25	116.1797	HC37	82.75742
P10	73.09549	P70	125.6758	PC26	83.49354	HC38	85.29345
P11	76.91577	P71	103.1216	PC27	152.4545	HC39	66.79669
P12	94.24408	P72	151.3794	PC28	74.69362	HC40	66.8395
P13	112.1623	P73	92.17244	PC29	40.04303	HC41	38.36233
P14	506.7169	P74	135.4018	PC30	78.97527	HC42	16.0046
P15	56.73929	P75	83.26516	PC31	181.0562	HC43	65.0591
P16	260.7952	P76	54.468	PC32	58.20785	HC44	10.70816
P17	118.0375	P77	104.0017	PC33	175.6915	HC45	61.40263
P18	113.7196	P78	82.72276	PC34	84.81707	HC46	79.25872
P19	116.4024	P79	74.18954	PC35	28.53753	HC47	33.70497
P20	114.138	P80	84.91162	PC36	60.55444	HC48	19.26087
P21	163.1362	P81	221.6661	PC37	96.69381	H1	58.274
P22	129.207	P82	102.1824	PC38	68.19497	H2	10.28781
P23	73.38303	P83	150.6566	PC39	201.4285	H3	35.58598
P24	80.87981	P84	143.861	PC40	58.56299	H4	82.57819
P25	87.13583	P85	96.33262	PC41	43.32241	H5	20.18925
P26	88.70023	P86	146.8978	PC42	64.25178	H6	420.606
P27	495.2097	P87	131.7254	PC43	213.1548	H7	33.35919
P28	154.7267	P88	62.75983	PC44	49.66521	H8	13.73727
P29	248.3447	P89	108.2097	PC45	148.2462	H9	96.46325
P30	131.3649	P90	88.42272	PC46	77.07405	H10	25.84206
P31	109.6578	P91	101.4337	PC47	32.78613	H11	515.6238
P32	150.38	P92	141.4801	PC48	52.81977	H12	40.0481
P33	83.04739	P93	212.7528	HC1	9.763956	H13	40.02574
P34	147.7877	P94	75.02004	HC2	46.3021	H14	94.67937
P35	138.5507	P95	118.8031	HC3	93.12263	H15	37.77152
P36	63.97963	P96	73.29417	HC4	79.58225	H16	1446.511
P37	61.92638	P97	112.4324	HC5	31.51563	H17	12.10141
P38	76.37237	P98	140.6511	HC6	23.36614	H18	10.86856
P39	93.26484	P99	100.4297	HC7	36.37113	H19	66.03481
P40	425.4877	P100	129.7038	HC8	26.42649	H20	35.46569
P41	150.7396	P101	75.70959	HC9	106.9796	H21	912.5966
P42	273.2536	P102	97.24219	HC10	32.17024	H22	30.53594
P43	111.6827	P103	100.7524	HC11	8.980914	H23	54.08551
P44	123.6851	P104	66.93466	HC12	10.16078	H24	83.48123
P45	75.50131	PC1	219.2818	HC13	40.31565	H25	93.1171
P46	89.86905	PC2	73.34705	HC14	73.36364	H26	1259.372
P47	127.6154	PC3	159.0904	HC15	132.7043	H27	44.84229
P48	110.2517	PC4	109.7359	HC16	14.60212	H28	20.55145
P49	100.9686	PC5	46.22369	HC17	17.87389	H29	49.30597

(Continued on next page)

Table 6. (Continued)

Output	LCA	Output	LCA	Output	LCA	Output	LCA
P50	93.59408	PC6	74.23904	HC18	23.33053	H30	29.96533
P51	66.77977	PC7	131.5831	HC19	72.54818	H31	1040.372
P52	83.86248	PC8	76.65914	HC20	85.61755	H32	9.936149
P53	51.59391	PC9	177.8157	HC21	67.01632	H33	13.44292
P54	57.57451	PC10	85.49307	HC22	59.6534	H34	91.56566
P55	235.7266	PC11	54.63544	HC23	8.913739	H35	97.1799
P56	122.7315	PC12	74.00226	HC24	8.724029	H36	546.6934
P57	145.1701	PC13	174.0626	HC25	58.63201	H37	31.6075
P58	119.8743	PC14	77.617	HC26	51.65626	H38	24.58541
P59	131.9668	PC15	198.3484	HC27	90.45776	H39	31.94526
P60	117.6084	PC16	99.57905	HC28	70.72826	H40	49.84941
						Minimum cost ($/h)	447,709.9

Table 7. Comparison of LCA with other methods for Testcase 3.

Method	Minimum cost ($/h)
CSO [32]	471,285.2852
NDIDE [53]	466,910
HNTMACSO [52]	466,165.5273
DRL-CSO [13]	464,509.3057
LCA	447,709.9232

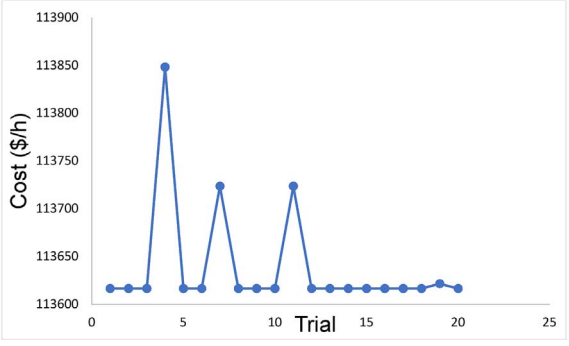

Figure 14. Best costs obtained in 20 trials of LCA.

Table 8. Performance of LCA compared to other methods.

Algorithms	Minimum cost ($/h)	Average cost ($/h)	Maximum cost ($/h)	SD	Execution time (s)
Testcase 1					
TVAC-PSO	117,824.8956	NA	NA	NA	44.82
OTLBO	116,579.239	116,613.6505	116,649.4473	NA	36.43
TVAC-GSA-PSO	117,438.6000	NA	NA	NA	6.94
SDEGCM	115,626.3697	115,703.4812	115,768.3882	41.5708	1308.61
DRL-CSO	115,952.904	116,051.472	116,170.447	54.523	29.53
FSRPSO	115,769.6300	NA	NA	NA	10.06
LCA	113,616.5734	113,639.1187	113,848.2036	59.147	26
Testcase 2					
CSO	233,663.273	233742.648	233,863.5784	43.9545	201.14
ISNS	233,543.659	234,,858.609	235,974.7405	522.741	NA
SADEGCM	231,590.4057	231913.386	232,251.5939	192.479	NA
IMPOA	235,260.3	NA	NA	NA	NA
DRL-CSO	233,326.532	233,416.174	233,529.94	162.975	58.26
LCA	220,107.797	220,224.573	221,292.7124	307	90
Testcase 3					
CSO	471,285.2852	471,795.4751	473,362.1462	517.4711	461.34
NDIDE	466,910	468,316	469,983	674	231.4
HNTMACSO	466,165.5273	467,215.4926	468,265.4578	506.3926	273.34
DRL-CSO	464,509.3057	465,515.282	465,842.3471	457.613	167.32
LCA	447,709.9232	448,122.5341	448,279.6019	985.1	180

Table 9. Wilcoxon signed rank test.

Testcase systems	α	p-value
Case 48	0.05	0.000001907
Case 96	0.05	0.00000197
Case192	0.05	0.000007629

optimum solutions for the objective function and enhanced the convergence rate of the algorithm. In order to assess the superiority of the bio-inspired LCA, 3 test systems were employed, where one is a 48-unit medium test system and two large-scale test systems, 96 and 192 units, are employed, considering valve point impacts for all power-only units. The applications underwent testing and implementation under power and heat-loading conditions. To assess the efficacy of the LCA technique, a comparison was conducted using recently developed algorithms. The simulation results indicate that the proposed LCA technique surpasses other algorithms in terms of performance. The simulation results of the LCA demonstrate that the proposed algorithm's performance remains unaffected by various nonlinearities resulting from valve point loading of thermal units, as well as the size of the system. This indicates the algorithm's robustness. The proposed strategy has the potential to enhance the rate of convergence and provide a solution that encompasses the whole problem space. Consequently, LCA has been successfully utilized to investigate CHPED concerns. From statistical analysis, it can be concluded that LCA exerts an excellent compromise between execution time and generation costs. The generation cost is reduced, and the time of execution is also less. It is also observed that the proposed algorithm consistently gives the best value. In future work, the use of the proposed algorithm may be implemented to solve the multiobjective CHP economic emission dispatch problem, including renewable energy sources.

References

1 Gowrishankar V., Angelides C., Druckenmiller H. (2013). *Combined heat and power systems: Improving the energy efficiency of our manufacturing plants, buildings, and other facilities*. NRDC Issue Paper 13-04-B. Available at https://www.nrdc.org/sites/default/files/combined-heat-power-IP.pdf.

2 Guo T., Henwood M.I., Van Ooijen M. (1996) An algorithm for combined heat and power economic dispatch. *IEEE Trans. Power Syst.* **11**, 1778–1784.

3 Rooijers F.J., Van Amerongen R.A. (1994) Static economic dispatch for co-generation systems, *IEEE Trans. Power Syst.* **9**, 1392–1398.

4 Rao P.S.N. (2006) Combined heat and power economic dispatch: A direct solution, *Electr. Power Compo. Syst.* **34**, 9, 1043–1056. https://doi.org/10.1080/15325000600596775.

5 Ohaegbuchi D.N., Maliki O.S., Okwaraoka C.P.A., Okwudiri H.E. (2022) Solution of combined heat and power economic dispatch problem using direct optimization algorithm, *Energy Power Eng.* **14**, 737–746. https://doi.org/10.4236/epe.2022.1412040.

6 Lahdelma R., Hakonen H. (2003) An efficient linear programming algorithm for combined heat and power production, *Eur. J. Oper. Res.* **148**, 1, 141–151. https://doi.org/10.1016/s0377-2217(02)00460-5.

7 Cho H., Luck R., Eksioglu S.D., Chamra L.M. (2009) Cost-optimized real-time operation of CHP systems, *Energy Build.* **41**, 4, 445–451. https://doi.org/10.1016/j.enbuild.2008.11.011.

8 Moradi Dalvand M., Nazari Heris M., Mohammadi Ivatloo B., Galavani S., Rabiee A. (2019) A two-stage mathematical programming approach for the solution of combined heat and power economic dispatch, *IEEE Syst. J.* **14**, 2, 2873–2881. https://doi.org/10.1109/JSYST.2019.2909627.

9 Shen Z., Wu C., Wang L., Zhang G. (2021) Real-time energy management for microgrid with EV station and CHP generation, *IEEE Trans. Netw. Sci. Eng.* **8**, 2, 1492–1501. https://doi.org/10.1109/tnse.2021.3062846.

10 Jour M.Y., Wang H., Hong F., Yang J., Chen Z., Cui H., Feng J. (2021) Modeling and optimization of combined heat and power with power-to-gas and carbon capture system in integrated energy system, *Energy* **236**, 121392. https://doi.org/10.1016/j.energy.2021.121392.

11 Eke İ. (2022) Combined heat and power economic dispatch by Taguchi-based filled function, *Eng. Optim.* **55**, 5, 791–805. https://doi.org/10.1080/0305215X.2022.2034802.

12 Zhou S., Hu Z., Gu W., Jiang M., Chen M., Hong Q., Booth C. (2020) Combined heat and power system intelligent economic dispatch: A deep reinforcement learning approach, *Int. J. Electr. Power Energy Syst.* **120**, 106016. https://doi.org/10.1016/j.ijepes.2020.106016.

13 Meng A., Rong J., Yin H., Luo J., Tang Y., Zhang H., Li C., Zhu J., Yin Y., Li H., Liu J. (2024) Solving large-scale combined heat and power economic dispatch problems by using deep reinforcement learning based crisscross optimization algorithm, *Appl. Therm. Eng.* **245**, 122781. https://doi.org/10.1016/j.applthermaleng.2024.122781.

14 Su C.T., Chiang C.L. (2004) An incorporated algorithm for combined heat and power economic dispatch, *Electr. Power Syst. Res.* **69**, 187–195.

15 Subbaraj P., Rengaraj R., Salivahanan S. (2009) Enhancement of combined heat and power economic dispatch using self-adaptive real-coded genetic algorithm, *Appl. Energy* **86**, 915–921.

16 Haghrah A., Nazari-Heris M., Mohammadi-Ivatloo B. (2016) Solving combined heat and power economic dispatch problem using real-coded genetic algorithm with improved Mühlenbein mutation, *Appl. Therm. Eng.* **99**, 465–475.

17 Chen X., Li K. (2022) Collective information-based particle swarm optimization for multi-fuel CHP economic dispatch problem, *Knowledge-Based Syst.* **248**, 108902.

18 Xiong G., Shuai M., Hu X. (2022) Combined heat and power economic emission dispatch using improved bare-bone multi-objective particle swarm optimization, *Energy* **244-B**, 123108.

19 Neto J.X.V., Reynoso-Meza G., Ruppel T.H., Mariani V.C., dos Santos Coelho, L. (2017) Solving non-smooth economic dispatch by a new combination of continuous GRASP algorithm and differential evolution, *Int. J. Electr. Power Energy Syst.* **84**, 13–24.

20 Chen X., Shen A. (2022) Self-adaptive differential evolution with Gaussian–Cauchy mutation for large-scale CHP economic dispatch problem, *Neural Comput. Appl.* **34**, 11769–11787. https://doi.org/10.1007/s00521-022-07068-w.

21 Basu M. (2015) Combined heat and power economic dispatch using opposition-based group search optimization, *Int. J. Electr. Power Energy Syst.* **73**, 819–829.

22 Davoodi E., Zare K., Babaei E. (2017) A GSO-based algorithm for combined heat and power dispatch problem with modified scrounger and ranger operators, *Appl. Therm. Eng.* **120**, 36–48.

23 Nguyen T.T., Vo D.N. (2015) The application of one rank cuckoo search algorithm for solving economic load dispatch problems, *Appl. Soft Comput.* **37**, 763–773. https://doi.org/10.1016/j.asoc.2015.09.010.

24 Jayakumar N., Subramanian S., Ganesan S., Elanchezhian E. (2015) Combined heat and power dispatch by grey wolf optimization. *Int. J. Energy Sector Manage.* **9**, 523–546.

25 Huang S.H., Lin P.C. (2013) A harmony-genetic based heuristic approach toward economic dispatching combined heat and power, *Int. J. Electr. Power Energy Syst.* **53**, 482–487.

26 Khorram E., Jaberipour M. (2011) Harmony search algorithm for solving combined heat and power economic dispatch problems, *Energy Convers. Manage.* **52**, 1550–1554.

27 Basu M. (2011) Bee colony optimization for combined heat and power economic dispatch, *Expert Syst. Appl.* **38**, 13527–13531.

28 Jayabarathi T., Yazdani A., Ramesh V., Raghunathan T. (2014) Combined heat and power economic dispatch problem using the invasive weed optimization algorithm, *Front. Energy* **8**, 25–30.

29 Roy P.K., Paul C., Sultana S. (2014) Oppositional teaching learning-based optimization approach for combined heat and power dispatch, *Int. J. Electr. Power Energy Syst.* **57**, 392–403.

30 Nasir M., Sadollah A., Aydilek İ.B., Lashkar Ara A., Nabavi-Niaki S.A. (2021) A combination of FA and SRPSO algorithm for combined heat and power economic dispatch, *Appl. Soft Comput.* **102**, 107088. https://doi.org/10.1016/j.asoc.2021.107088.

31 Meng A.-B., Chen Y.-C., Yin H., Chen S.-Z. (2014) Crisscross optimization algorithm and its application, *Knowledge-Based Syst.* **67**, 218–229.

32 Meng A., Mei P., Yin H., Peng X., Guo Z. (2015) Crisscross optimization algorithm for solving combined heat and power economic dispatch problem, *Energy Convers. Manage.* **105**, 1303–1317. https://doi.org/10.1016/j.enconman.2015.09.003.

33 Mirjalili S., Mirjalili S.M., Hatamlou A. (2016) Multi-verse optimizer: A nature-inspired algorithm for global optimization, *Neural Comput. Appl.* **27**, 495–513. https://doi.org/10.1007/s00521-015-1870-7.

34 Shaheen A.M., Elsayed A.M., Ginidi A.R., El-Sehiemy R.A., Alharthi M.M., Ghoneim S.S.M. (2022) A novel improved marine predators algorithm for combined heat and power economic dispatch problem, *Alex. Eng. J.* **61**, 3, 1834–1851. https://doi.org/10.1016/j.aej.2021.07.001.

35 Rizk-Allah R.M., Hassanien A.E., Snasel V. (2022) A hybrid chameleon swarm algorithm with superiority of feasible solutions for optimal combined heat and power economic dispatch problem, *Energy* **254**, 124340. https://doi.org/10.1016/j.energy.2022.124340.

36 Ramachandran M., Mirjalili S., Nazari-Heris M., Parvathysankar D.S., Sundaram A., Gnanakkan C.A.R. (2022) A hybrid grasshopper optimization algorithm and Harris Hawks optimizer for combined heat and power economic dispatch problem, *Eng. Appl. Artif. Intell.* **111**, 104753. https://doi.org/10.1016/j.engappai.2022.104753.

37 Gafar M., Ginidi A., El-Sehiemy R., Sarhan S. (2022) Improved SNS algorithm with high exploitative strategy for dynamic combined heat and power dispatch in co-generation systems, *Energy Rep.* **8**, 8857–8873. https://doi.org/10.1016/j.egyr.2022.06.054.

38 Nazari A., Abdi H. (2022) Solving the combined heat and power economic dispatch problem in multi-zone systems by applying the imperialist competitive Harris hawks optimization, *Appl. Soft Comput.* **26**, 12461–12479. https://doi.org/10.1007/s00500-022-07159-9.

39 Wolpert D.H., Macready W.G. (1997) No free lunch theorems for optimization, *IEEE Trans. Evol. Comput.* **1**, 1, 67–82. https://doi.org/10.1109/4235.585893.

40 Decker G.L., Brooks A.D. (1958) Valve point loading of turbines, *Trans. Am. Inst. Electr. Eng. Power Apparatus Syst.* **77**, 481–484.

41 Pulluri H., Kumar N.G., Rao U.M., Preeti, Kumar M.G. (2019) Krill herd algorithm for solution of economic dispatch with valve-point loading effect, in: *Applications of computing, automation and wireless systems in electrical engineering*, Vol. **553**, Springer, pp. 431–440. https://doi.org/10.1007/978-981-13-6772-4_33.

42 Houssein E.H., Oliva D., Abdel Samee N., Mahmoud N.F., Emam M.M. (2023) Liver Cancer Algorithm: A novel bio-inspired optimizer, *Comput. Biol. Med.* **165**, 107389. https://doi.org/10.1016/j.compbiomed.2023.107389.

43 Feldman J.P., Goldwasser R., Mark S., Schwartz J., Orion I. (2009) A mathematical model for tumor volume evaluation using two-dimensions, *J. Appl. Quant. Methods* **4**, 4, 455–462.

44 Sápi J., Kovács L., Drexler D.A., Kocsis P., Gajári D., Sápi Z. (2015) Tumor volume estimation and quasi-continuous administration for most effective bevacizumab therapy, *PLoS One* **10**, 11, e0142190.

45 Vatandoust S., Price T.J., Karapetis C.S. (2015) Colorectal cancer: Metastases to a single organ, *World J. Gastroenterol.* **21**, 41, 11767. https://doi.org/10.3748/wjg.v21.i41.11767.

46 Mahender K., Srinivasa Rao G., Kamalakar G., Venkateshwarlu S., Polasa S., Pulluri H. (2025) Optimizing combined heat and power economic dispatch using a differential evolution algorithm, in *Proceedings of the Second International Conference on Renewable Energy, Green Computing and Sustainable Development (ICREGCSD 2025)*, pp. 1–9. https://doi.org/10.1051/e3sconf/202561602025.

47 Pulluri H., Basetti V., Goud B.S., Naga Sai Kalyan C. (2024) Exploring evolutionary algorithms for optimal power flow: A comprehensive review and analysis, *Electricity* **5**, 4, 712–733. https://doi.org/10.3390/electricity5040035.

48 Beigvand S.D., Abdi H., La Scala M. (2016) Combined heat and power economic dispatch problem using gravitational search algorithm, *Electr. Power Syst. Res.* **133**, 160–172. https://doi.org/10.1016/j.epsr.2015.10.007.

49 Mohammadi-Ivatloo B., Moradi-Dalvand M., Rabiee A. (2013) Combined heat and power economic dispatch problem solution using particle swarm optimization with time varying acceleration coefficients, *Electr. Power Syst. Res.* **95**, 9–18. https://doi.org/10.1016/j.epsr.2012.08.005.

50 Beigvand S.D., Abdi H., La Scala M. (2017) Hybrid gravitational search algorithm–particle swarm optimization with time varying acceleration coefficients for large scale CHPED problem, *Energy* **126**, 841–853.

51 Nazari-Heris M., Mehdinejad M., Mohammadi-Ivatloo B., Abapour M. (2017) Combined heat and power economic dispatch problem solution by implementation of whale optimization method, *Neural Comput. Appl.* **31**, 421–436. https://doi.org/10.1007/s00521-017-3074-9.

52 Zhou T., Chen J., Xu X., Ou Z., Yin H., Luo J., Meng A. (2023) A novel multi-agent based crisscross algorithm with hybrid neighboring topology for combined heat and power economic dispatch, *Appl. Energy* **342**, 121167.

53 Liu D., Hu Z., Su Q. (2022) Neighborhood-based differential evolution algorithm with direction induced strategy for the large-scale combined heat and power economic dispatch problem, *Inform. Sci.* **613**, 469–493. https://doi.org/10.1016/j.eswa.2022.119438.